

Assessment of custom in-situ electrodes for the chemical
analysis of a coastal salt pond and other extreme
environments

A Senior Honors Thesis for the Department of Chemistry

By

Jessica Stephanie Dabrowski

Tufts University

May 2017

Table of Contents

Acknowledgements.....	5
Abstract.....	6
Introduction.....	7
Experimental.....	17
1. Materials.....	17
2. Electrode development.....	19
2a. Standard calibration of ion-selective electrodes.....	20
2b. Construction of liquid filled electrodes.....	20
2c. Construction and characterization of WCL electrodes.....	21
2d. Construction and characterization of Newly-Designed (ND) electrodes.....	24
3. Testing and preparation for in-situ measurements.....	28
3a. Calibrations under expected conditions – sulfidic, anoxic and mixed solutions.....	28
3b. Analysis of real samples - Skaftá subglacial lakes.....	29
3c. Tests of array and commercial sulfide electrode in seawater simulants.....	30
3d. Temperature probe test.....	32
3e. Pressure conditioning.....	32
4. In-situ measurements at Oyster Pond.....	34
4a. Instrumentation and electronics.....	34
4b. Field site description, in-situ data collection, and sampling.....	35

5. In-lab analysis of Oyster Pond samples	37
5a. Conductivity and pH.....	37
5b. ICP-AES	38
5c. Ion chromatography (IC)	39
Results.....	41
1. Preparation and testing for in-situ measurements	41
1a. Calibrations under expected conditions – sulfidic and anoxic	41
1b. Analysis of real samples - Skaftá subglacial lakes	45
1c. Tests of array and commercial sulfide electrode in seawater simulants.....	45
2. In-situ measurements at Oyster Pond.....	48
2a. First expedition: July 29 th , 2016	48
2b. Electrode adjustments: Sulfide ISE characterization and pressure conditioning of electrodes.....	52
2c. Second expedition: August 28 th , 2016.....	53
3. In-lab analysis of Oyster Pond samples	59
3a. Conductivity and pH results	59
3b. ICP-AES results.....	60
3c. Ion chromatography results	61
Discussion.....	65
1. Evaluation of tests for “field-readiness”	65

2. In-situ measurements at Oyster Pond.....	68
3. Comparison of in-situ to in-lab analysis and interpretation of Oyster Pond’s chemistry	70
Conclusion	76
Supplemental.....	78
WCL electrodes characterization.....	78
Calibrations under expected conditions and Skaftá sample measurements	79
ND ISEs characterization	80
In-situ measurements at Oyster Pond	80
In-lab analysis of samples.....	83
Table of Figures	84
References.....	87

Acknowledgements

I would like to acknowledge and thank several important people, without whom I would not have completed this thesis. Elizabeth Oberlin, my mentor and fellow researcher in the Kounaves Lab, was irreplaceable in her guidance in the laboratory and in the field. I would like to thank her for help with my writing, with brainstorming, and for always being there when I needed someone to talk to. I would also like to thank Andrew Weber for teaching me about the wonders of ion-selective electrodes. I also acknowledge the other lab members for their assistance during my two years in the group. I am also grateful for the guidance, support and everlasting enthusiasm from Professor Kounaves as a research advisor. I also want to give thanks to Alexander Elmer for help with fieldwork and construction of the pulley system. I acknowledge Kurt Hanselmann for showing me around Woods Hole and helping me contact OPET. I would also like to thank Bill Kerfoot and OPET for allowing me to borrow boating equipment and for being so accommodating while I was in Falmouth.

This project would not have been possible without the funding and support of the Arnold O. Mabel Beckman Foundation and Tufts University. Thank you for choosing to support me as a young Beckman Scholar. I am grateful for the enthusiasm and support of Professor Kritzer during my time as a Beckman Scholar. And finally, thank you to my advisors, Professor Thomas and Professor Ridge, and my friends at Tufts that were always there to listen and lend a hand.

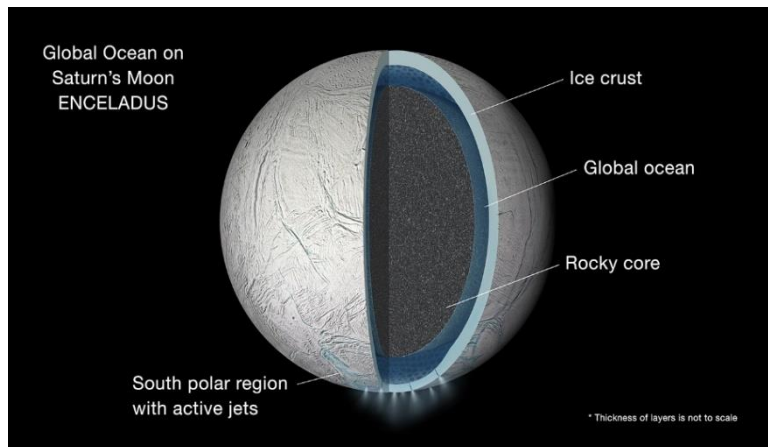
Abstract

The purpose of this study was to evaluate a novel array of ion-selective electrodes (ND ISEs) for future in-situ chemical analysis of extreme environments such as the subsurface oceans of Europa and Enceladus, moons of Jupiter and Saturn, respectively, and the Skaftá subglacial lakes in Iceland. The well-studied model system of Oyster Pond (Falmouth, MA) was used as an analogous environment for evaluation of the in-situ technique since it was known to be anoxic and contain sulfide,¹ like the Skaftá lakes.² The ISEs could withstand sulfidic, anoxic, and high pressure conditions. Their fast response and selectivity allowed for fast, real-time in-situ data collection. The standard techniques (ion chromatography and ICP-AES) did not measure the “free” activity of the ions in the natural environment, and were much more tedious in sample collection, storage, preparation and analysis. In contrast, the ND ISEs allowed for nearly instantaneous data collection in the real environment without the need for any sample alteration. For future analyses, it would be necessary to test larger batches of ISEs to choose the most-field ready electrodes, to incorporate more channels in the potentiometer in case of failure, and to research sulfide poisoning of anion-selective ISEs further.

Introduction

The search for life in the solar system is currently focused on finding habitats that contain water, the main ingredient for life.³ Subsurface oceans on Europa and Enceladus are two major examples of environments that may support life. Both of these moons, of Jupiter and Saturn, respectively, are thought to have oceans beneath their icy crusts due to geologic activity that maintains water in a liquid form (Figure 1).⁴

Knowing whether these environments are habitable would require studying the chemistry these oceans. Unfortunately, these



satellites are difficult and expensive to study, but analogues on Earth may provide insight into the habitability and potential sources of energy for life in these extreme environments as well as serve as test sites for instrumentation we might send to these moons.

The Skaftá lakes beneath the Vatnajökull ice cap in Iceland share many characteristics with the extraterrestrial subsurface oceans, including isolation from the atmosphere by a thick layer of ice and influence from volcanic activity, producing an anoxic environment containing high levels of sulfide.⁵ Despite the extreme conditions, life still flourishes in these lakes that is substantially different from nearby environments. The microbes in this environment do not experience sunlight, so they must rely on chemical energy to survive.^{2,6} Similar conditions are expected for life on Enceladus, so understanding the chemistry of the Skaftá lakes would inform scientists on whether the chemical environment of Enceladus is habitable.

Previous studies of the Skaftá lakes involved numerous challenges. Because the lakes are overlain by 200-300 meters of ice, drilling a borehole to reach the lakes took 12 hours and resulted in a maximum borehole diameter of 10 centimeters, quite a small diameter for any instrument or sampling bottle, limiting the obtainable amount of sample.^{2,6,7} Gaidos et al. (2009) only obtained one sample

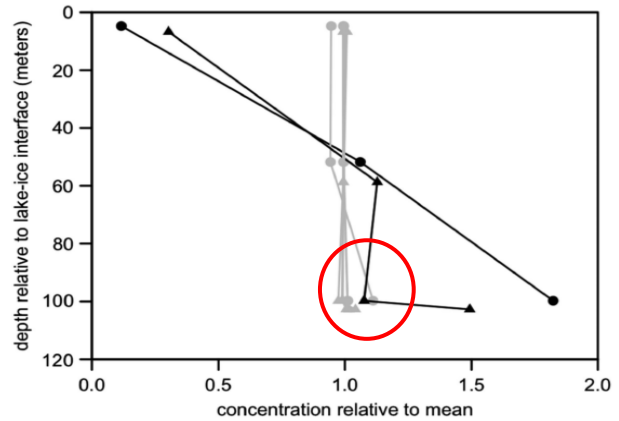


Figure 2. Ion profiles in the East Skaftá Lake. The triangle and circle represent 2 different boreholes. Sulfate is in black. SiO₂, Na⁺ and Cl⁻ are in gray. (Adapted from Marteinsson et al. 2013).

from the West Skaftá lake. Marteinsson et al. (2013) also had limited success in collecting samples and data. Figure 2 demonstrates that they were only able to collect 4 samples beneath each borehole and at 50-meter intervals. Also, the sulfate profiles underneath one of the boreholes shows a significant difference within a few meters, which could be extraneous data, but without more samples, it's not possible to eliminate this point. The authors also reported degassing of the samples they brought to the surface, specifically of CO₂ and H₂S, which causes chemical changes in the sample. An in-situ technique would solve many of these issues by measuring chemical properties in real time in the environment and collect thousands of data points in the water column with a fast-enough response time.

Evaluation and testing of an in-situ technique requires an accessible yet chemically similar environment to the Skaftá lakes and Enceladus. This environment should also be well studied. Oyster Pond, a coastal pond in Falmouth, MA, less than two hours away from Boston, is both anoxic and sulfidic¹ like the Skaftá lakes. This pond was used as a model system for oceanographic

methods in the 1960s and has been carefully monitored since the late 1980s due to the economic importance of the pond to the surrounding residents and ecological systems.¹

This brackish coastal pond receives freshwater, from precipitation, runoff and groundwater, and seawater during the highest tides, especially during storm surges.¹ The connection to the ocean is through a lagoon and Trunk River with a total channel length of about 100 meters (Figure 3). The difference in density between the salty and fresh waters causes a saline bottom layer to form. Typical wind currents in the pond have been found to only mix the upper 4 meters of the water column in the past. The two main basins of the pond, the northern and southern basins, have different depths of ~4.5 and ~6.5 meters, respectively. The shallower, northern basin was found to be seasonally anoxic and was shallow enough to mix thoroughly in the winter. The deeper, southern basin has been more stratified and permanently anoxic at the bottom, likely due to the greater influence of seawater and deeper water column (Figure 4).¹

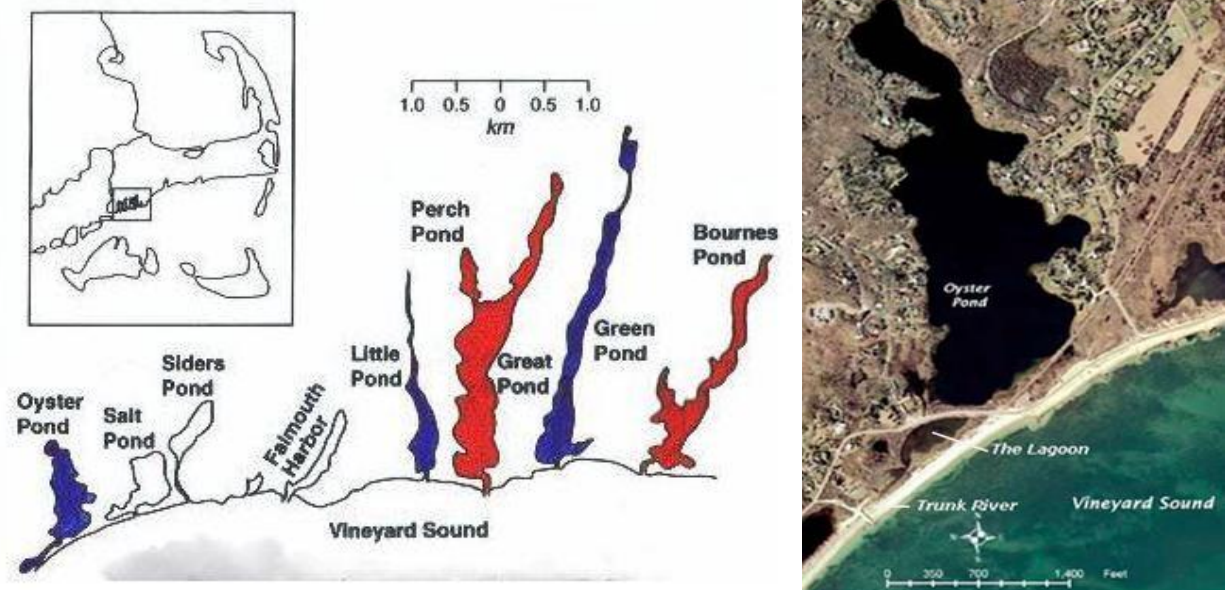


Figure 3. A map showing the location of Oyster Pond in southern Massachusetts and details of the connection to the Vineyard Sound through the Lagoon and Trunk River. (Courtesy of OPET, Inc.)⁸

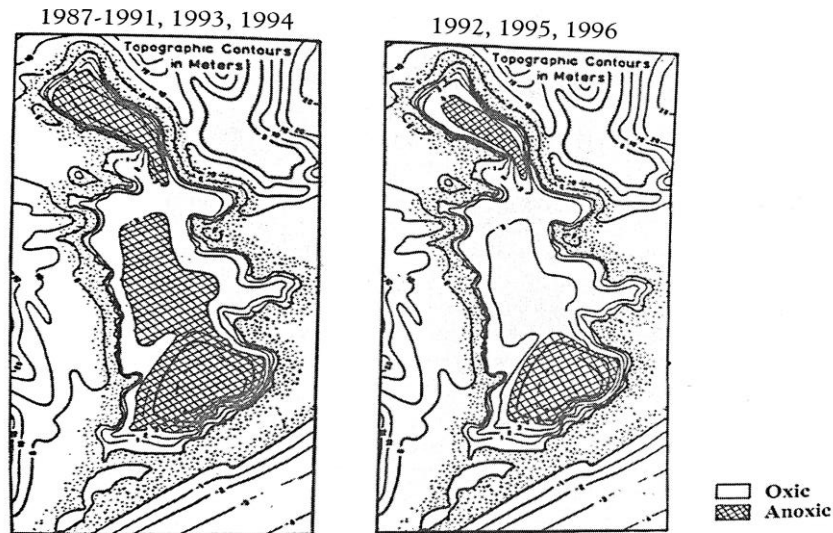


Figure 4. Historic anoxia in Oyster Pond. The diagram on the right was under lower salinity conditions. (From Emery et al. 1997)

The salinity and ecological state of the pond has varied substantially over its history. In the 19th century, it had a more direct tidal inlet to the sound, so it was essentially an estuary. From 1948 to 1986, it was stable and brackish with a much lower salinity of 2-4 ppt, compared to the Sound's salinity of 32 ppt. The salinity increased in the late 1980s to 15-20 ppt (Figure 5) due to increased dredging of the

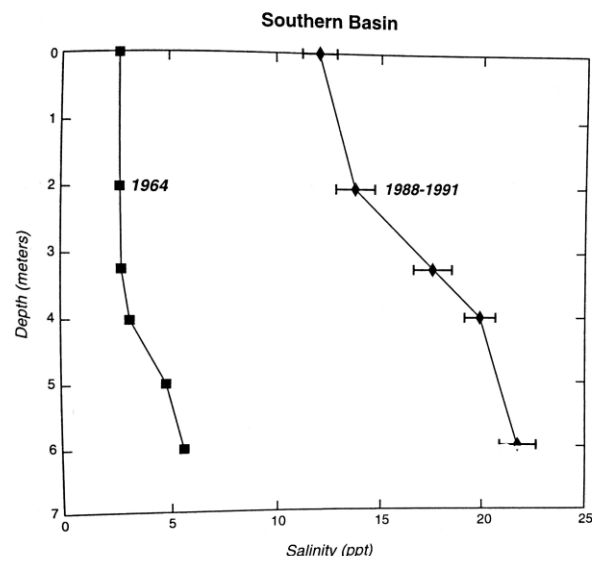


Figure 5. The salinity as a function of depth in the southern, deeper basin of Oyster Pond as reported by Emery (1964) and Howes and Hart (1988-1991).¹

tidal channel and caused water lily and fish populations to decline.^{1,8} It was suspected that the increased dredging allowed for more seawater to enter the pond, increasing the stratification of the water layers. The steeper salinity and density gradient decreased the amount of mixing in the pond.

The lack of mixing caused anoxic zones at the bottom of the pond to expand, decreasing available benthic habitat for plant and animal biota. Sulfate-reducing microbes in the anoxic zones also produced sulfide, which also added to the uninhabitability of these zones.¹

The “decline” of this pond led to the creation of a management plan in the 1990s to keep the pond in a more stable state, comparable to the brackish conditions observed by Emery in the 1960s. The tidal input has been controlled using a dam and periodic dredging of the inlet as deemed necessary by water quality monitoring (Oyster Pond Environmental Trust, Inc. Pond Watchers and Water Quality Monitoring Program).^{1,8} In addition to the salinity and anoxia, nitrogen in the form of nitrate and ammonium has been carefully monitored because of the residential population and septic system issues.^{1,8} Because salinity, ammonium, and other chemical species have been well monitored in this pond, it is an excellent model system for assessing a new in-situ technique.

A type of in-situ method that would suit this aqueous environment well in addition to having the potential for measurements in space is potentiometry in the form of ion-selective electrodes (ISEs), such as the ones deployed on the Mars Phoenix Lander as part of the Wet Chemistry Lab (WCL).⁹ ISEs have excellent potential for in-situ analysis because of their ability to detect a variety of analytes with minimal power, volume, and mass requirements, as well as their fast response rates and real-time reporting of data, allowing for high resolution data to be collected with depth.^{9,10}

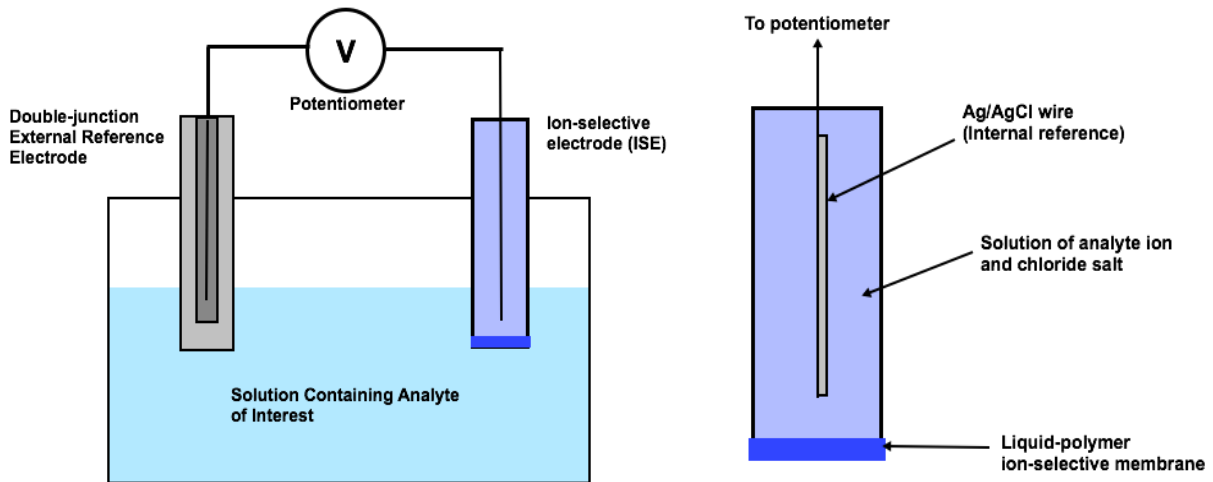


Figure 6. A typical potentiometric setup and details of a polymeric membrane-based ion-selective electrode. (Adapted from Harris 2007)

Potentiometry is a technique that measures electrochemical potential under zero-current conditions.^{10,11} Figure 6 shows a typical potentiometric setup with a reference electrode, ISE and potentiometer. The potentiometer measures the potential difference between the reference electrode, which should hold a stable potential regardless of the solution's composition, and the ISE which responds to the amount of analyte ion in the solution.¹⁰ The main components of a typical polymeric membrane ISE are also shown in Figure 6. A typical potentiometric setup and details of a polymeric membrane-based ion-selective electrode. (Adapted from Harris 2007) . The chemical potential at the membrane surface is transferred to the inner-filling solution of the ISE because it contains the analyte ion.¹² The chemical potential in the solution is transduced to an electronic potential by conversion of Cl^- to AgCl .¹³ The silver wire has an electrical response that is recorded by the potentiometer.

ISEs ideally respond to the activity of an ion in solution according to the Nernst Equation:

$$E = E^\circ + \frac{RT}{z_1 F} \ln a_I \quad (\text{Equation 1})$$

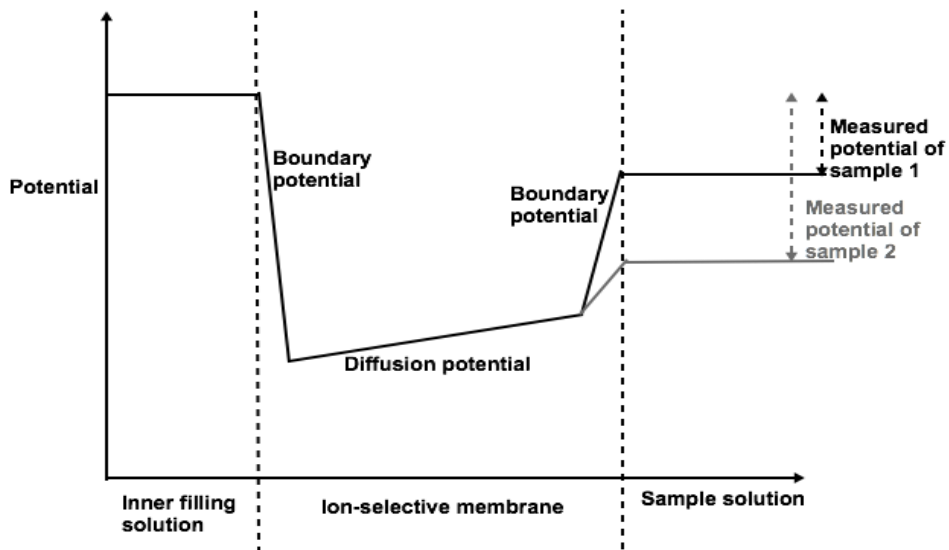
in which E is the measured electrode potential, E° is the standard value of the potential that includes sample-independent contributions, R is the gas constant, T is the temperature in Kelvin, F is Faraday's constant, z_i is the charge of the primary analyte ion, and a_i is the activity of the ion. The ideal slope is 59 mV/ z at 298 K for a decade increase in activity of the ion.^{10,14}

The activity is proportional to concentration, c , by an activity coefficient, γ as shown in Equation 2.¹³

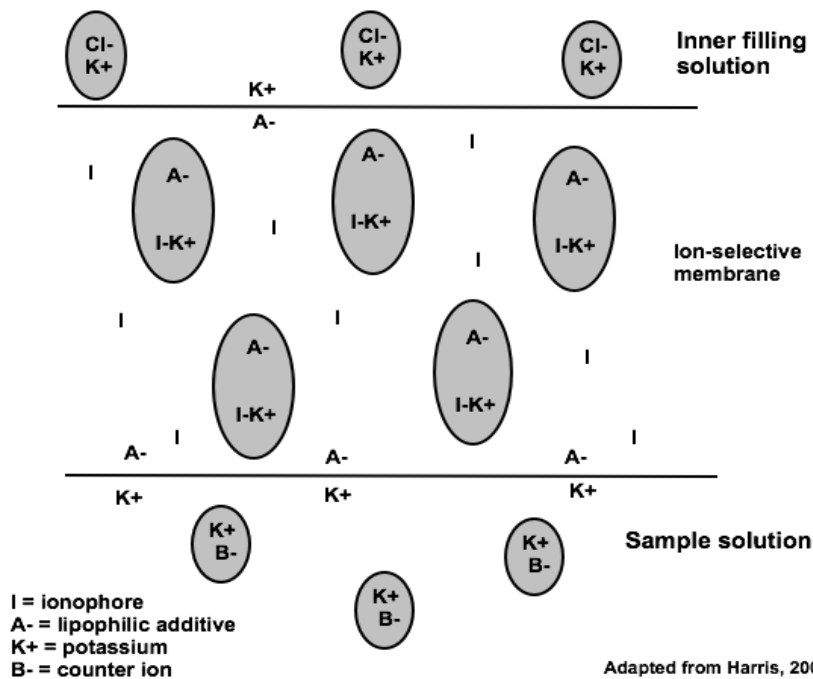
$$a = \gamma c \quad \text{(Equation 2)}$$

This coefficient depends on the ion radius and the ionic strength of the solution. In polymeric membrane-based ISEs, such as the ones used in this study, the ideal response of the electrode requires a constant composition of the membrane surface and selective complexation of the primary analyte ion by a ligand, known as an ion carrier or ionophore. These ionophores are typically hydrophobic, so that they prefer to remain dissolved in the polymer membrane rather than in an aqueous solution. A lipophilic salt is also added to the membrane to provide ion-exchange sites. This salt also functions to help increase the selectivity and lifetime of the ionophore.¹⁴

Figure 7 shows a schematic of the ionophore and additive dispersed in a K^+ -selective polymeric membrane. The sample solution creates a certain boundary potential at the surface of the membrane due to interaction with the additive and complexation with ionophore in the membrane. Because the concentration of the inner filling solution remains constant, the potential at this surface is also constant. The graph shows a mathematical representation of this phenomenon and how samples with different analyte concentrations produce a different measured potential. The diffusion potential should remain constant if the membrane has a constant composition.



Adapted from Mikhelson, 2013



Adapted from Harris, 2007

Figure 7. Components of the membrane potential. A graph of the components of the measured potential in an ion-selective electrode (top) and a detailed schematic of the components of a polymeric membrane (bottom).^{11,13}

The ion-selective electrodes prepared for the analysis of Oyster Pond and the Skaftá lakes included Na^+ , K^+ , Mg^{2+} , Ca^{2+} , and Cl^- electrodes because these ions are major components of seawater and aquatic systems influenced by hydrothermal fluids.^{15,16} A general anion ISE that responds the greatest to NO_3^- , based on the Hofmeister series,^{9,12} and NH_4^+ -selective electrode were also included because of the potential nitrogen enrichment of Oyster Pond due to septic leakage¹ and biological importance of nitrogen in these forms. For successful use as in-situ instruments, the ISEs must fulfill the following requirements:

- Selective for primary analyte
- No interference from the expected sulfide, anoxic conditions, mixed solutions
- Fast response time to allow for collection of many data points and high resolution depth profiles
- Sensitive to changes in concentration
- Working range of at least $10\ \mu\text{M}$ to $0.1\ \text{M}$ as expected in Oyster Pond and the Skaftá lakes
- Robust – can withstand pressure changes, exposure to muddy sediments and unfiltered water
- Stable and reproducible measurements

Batch water samples were collected in addition to in-situ data during this study to validate the technique. The standard lab methods of inductively-coupled plasma atomic emission spectroscopy (ICP-AES) and ion chromatography (IC) were compared to the results of the in-situ measurements and the known chemistry of Oyster Pond.

In addition to the new scientific knowledge about this technique, a comprehensive study of the major ions in seawater, ammonium and sulfide in this pond will benefit both the scientific community and the local community. Knowledge about mixing in the pond and the depth of the

anoxic layer is important for knowing the availability of the benthic environment to fish and other aquatic life and the patterns of salinity throughout the water column. Development and assessment of novel in-situ instrumentation for this anoxic and sulfidic environment will also provide new tools for the scientific community to use in chemical analysis of other coastal ponds, as well as the Skaftá lakes and extraterrestrial environments with further improvements.

Experimental

1. Materials

The materials used for the electrode membranes were sourced from with Fluka, A.G. Scientific or Sigma-Aldrich and included Sodium Ionophore X, Valinomycin (Potassium Ionophore I), Calcium Ionophore IV, Magnesium Ionophore VI, and Chloride Ionophore II. The additives included potassium tetrakis(p-chlorophenyl)borate (KTPCIPB), tridodecylmethylammonium nitrate (TDMAN), and tridodecylmethylammonium chloride (TDMAC), all from Fluka. The plasticizers for these membranes were bis-(2-ethylhexyl) sebacate (DOS) and 2-nitrophenyl octyl ether (o-NPOE) sourced from Acros Organics and Fluka. The polymer used in all membranes was high molecular weight polyvinyl chloride (PVC) from Fluka. The solvent for the membrane cocktails was tetrahydrofuran (THF) from Sigma-Aldrich. All membrane cocktails were found in the literature and recommended by Sigma-Aldrich as part of the Selectophore series and were chosen for their high selectivity for the primary analyte, except in the case of the nitrate electrode which was simply an anion-selective electrode. It was called a nitrate electrode because it is most selective for nitrate based on the Hofmeister series.¹² The approximate ratios of the membrane components are listed in Table 1 along with the appropriate reference. Approximately 100 mg of the membrane components were dissolved in 750-1500 μL of THF, depending on the viscosity needed. More dilute solutions were used in drop-casting to prevent bubble formation. After membrane application, all ISEs were conditioned in a 1-100 mM solution of the primary analyte.

Table 1. The membrane cocktails used for the constructed ion-selective electrodes

Primary Analyte Ion	Cocktail (% by weight) $\pm 1\%$	Reference
Calcium	1.0% Calcium ionophore IV 0.3% KTpCIPB 65.8% o-NPOE 32.9% PVC	Gehrig <i>et al.</i> , 1989 ¹⁷
Chloride	2% Chloride ionophore II $\leq 0.1\%$ TDMAC 65.0% DOS 33.0% PVC	Rothmaier and Simon, 1993 ¹⁸
Magnesium	1.0% Magnesium ionophore VI 0.7% KTpCIPB 65.6% o-NPOE 32.7% PVC	O'Donnell <i>et al.</i> , 1993 ¹⁹
Nitrate (Hofmeister Series¹²)	5-6% TDMAN 32% PVC 62% o-NPOE	Kounaves Lab Members, personal correspondence
Potassium	1.1% Potassium ionophore I 0.5% KTpCIPB 65.8% DOS 32.7% PVC	Qin <i>et al.</i> , 2000 ²⁰
Sodium	0.7% Sodium ionophore X 0.2% KTpCIPB 66.1% o-NPOE 33.0% PVC	Cadogen <i>et al.</i> , 1989 ²¹

The silver wire inside of the electrodes had a 1.0 mm diameter and was of 99.999% purity from VWR. A non-conductive epoxy (EPOTEK 730) was used to secure the silver wire to the housing. Heat-shrink and a rubber coating (Plasti-Dip®) from McMaster-Carr was used to cover all electrical connections. The electrodes were filed with a hydrogel made of 2,2-dimethoxy-2-phenyl-acetophenone (DMPAP) from Fluka and 2-hydroxyethyl methacrylate (HEMA) from Acros Organics. The Subglacial Lake (SGL) housings were made of Type 1 chemically-resistant PVC from McMaster-Carr. The WCL housings were made from Ultem (McMaster-Carr), a polymer that does not dissolve in THF.

All aqueous solutions were made using 18.2 M Ω deionized water (Barnstead Nanopure System). All inorganic salts were ACS Reagent Grade and obtained from Sigma-Aldrich or Fluka.

Volumetric flasks and an analytical balance were used to make solutions whenever possible to ensure the highest certainty in the concentrations.

The reference electrode used in all calibrations was a double-junction Orion™ reference electrode (Thermo Fisher Scientific). This reference electrode depends on the Ag/AgCl redox couple. The inner-filling solution was a saturated KCl solution provided by the manufacturer. The outer-filling solution was a neutral solution of 1.5 M lithium acetate. This electrolyte was used because neither lithium nor acetate are part of the chemical analysis, so any leaching of the outer-filling into the sample solution would not affect the analysis. For the in-lab analysis, a Lawson Labs, Inc. EMF16 potentiometer was used to collect data from the electrodes. This potentiometer was modified as described below for in situ analysis.

2. Electrode development

The array of ISEs must fulfill certain requirements before deployment in the environment. The first is that the electrodes are specific and responds to the ion of interest without significant interferences from other ions. The ISEs must also respond to the ion of interest within the range of concentrations expected within the environment. In this case, the electrodes should work in salinities similar to seawater and dilutions of 10 to 100 times that of seawater. The minimum was set to 100 times more dilute than seawater because Oyster Pond is about 15-30 times more dilute than Vineyard Sound at the surface.^{1,8} Because the goal of the study is to monitor stratification of ions in the water column, the electrodes must be sensitive to small changes in concentration. Finally, the electrodes must be robust enough to withstand handling and transport, exposure to muddy lake sediments, and the high pressures experienced in deep water. The maximum depth is about 7 meters, so the pressure on the electrodes nearly doubles from 1 atmosphere to 2

atmospheres between the surface and the bottom of the pond.²² Calibrations and tests of the electrodes were designed with these requirements in mind, as summarized below:

- Selective for primary analyte in seawater simulants
- Working range of 10 μM to 0.1 M
- Sensitive to analyte (large enough slopes in calibrations)
- Water-tight and pressure resistant to at least 2 atm

2a. Standard calibration of ion-selective electrodes

Unless otherwise noted, the calibrations of the ISEs were performed in a beaker of stirring deionized water. A small magnetic stir bar on a stir plate was used to stir the solution. Solutions of known salt concentrations were added to a known volume of water while stirring. The ISEs were allowed to reach a stable potential before increasing the concentration. The potential was averaged over the most stable portion of the response for data analysis.

2b. Construction of liquid filled electrodes

Typical liquid-filled ISEs were constructed for some experiments to test the membrane reagents. A typical ISE includes an electrode body, a silver wire coated with AgCl, a filling solution of a chloride salt and the analyte ion, and a liquid polymer selective membrane (Figure 8).^{11,13} First, the membrane cocktail is poured into a mold to create a master membrane. Then smaller discs are punched out of the master and applied to the body,

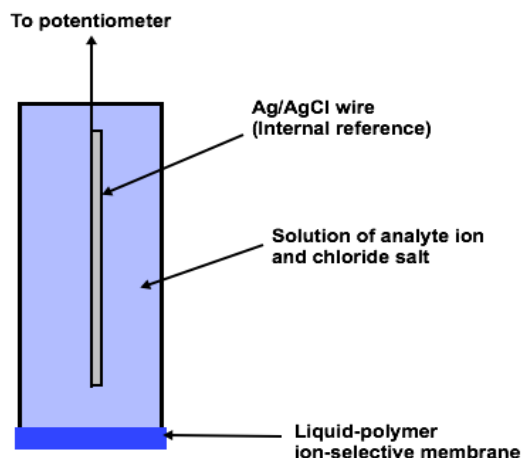


Figure 8. A cross-section of a typical ion-selective electrode

Tygon tubing made of mostly PVC. THF is used to dissolve the body and the membrane, creating a chemical seal once the THF evaporates. The silver wire is then anodized and inserted through the back of the body. The electrode is filled with the aqueous solution and then sealed.

2c. Construction and characterization of WCL electrodes

The Wet Chemistry Lab (WCL) ISEs were constructed as described in the procedures for the Phoenix Lander Mission.

Figure 9 is a cross-section of a WCL ISE.⁹

First, a silver wire was sanded flat on one end using fine sandpaper. The flat end of the silver wire was then inserted into the back of the inner housing shown in brown in Figure 9 and

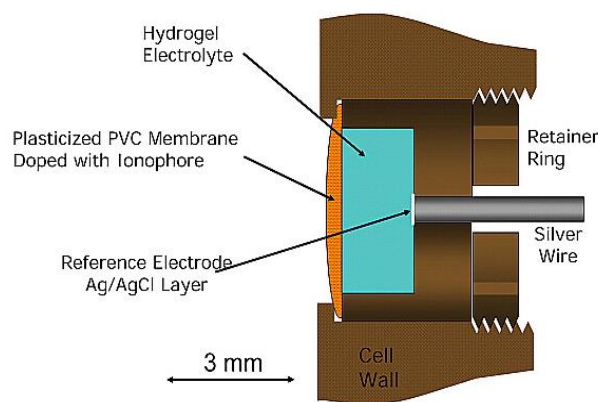


Figure 9. A cross-section of a WCL ion-selective electrode (Kounaves et al. 2009).

secured with non-conductive epoxy. The exposed surface of the silver wire was then anodized in 1 M KCl to plate a silver chloride layer onto the surface of the wire. The Ag/AgCl redox couple served as an internal reference. The well of the inner housing was then filled with a solution of 50% hydrogel (ratio of 20.0 mg of DMPAP to 1000. μ L of HEMA) and 50% of a 1 mM solution of the primary analyte ion and chloride. This solution was polymerized with UV light for a few minutes to form a semi-solid gel. The electrodes were then allowed to soak in the same electrolyte solution it was filled with. The last step is application of the membrane solution by drop-casting. Drop-casting is the act of putting a few drops of the membrane solution onto the electrode surface and allowing it to dry before applying another layer. Enough layers were applied to form a dome-like shape of membrane on the surface, depicted in orange in Figure 9. The inner housing was then

screwed into the outer housing and held with a retainer ring to physically seal the membrane to the rest of the electrode.

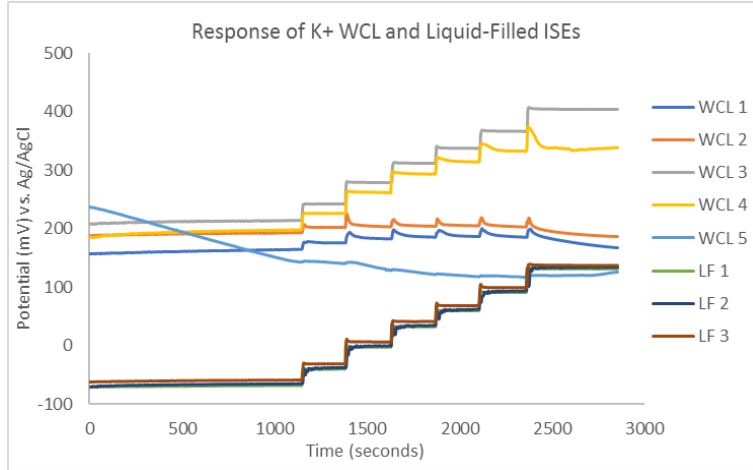


Figure 10. The response of K⁺-selective WCL and Liquid-Filled ISEs made with the same membrane components.

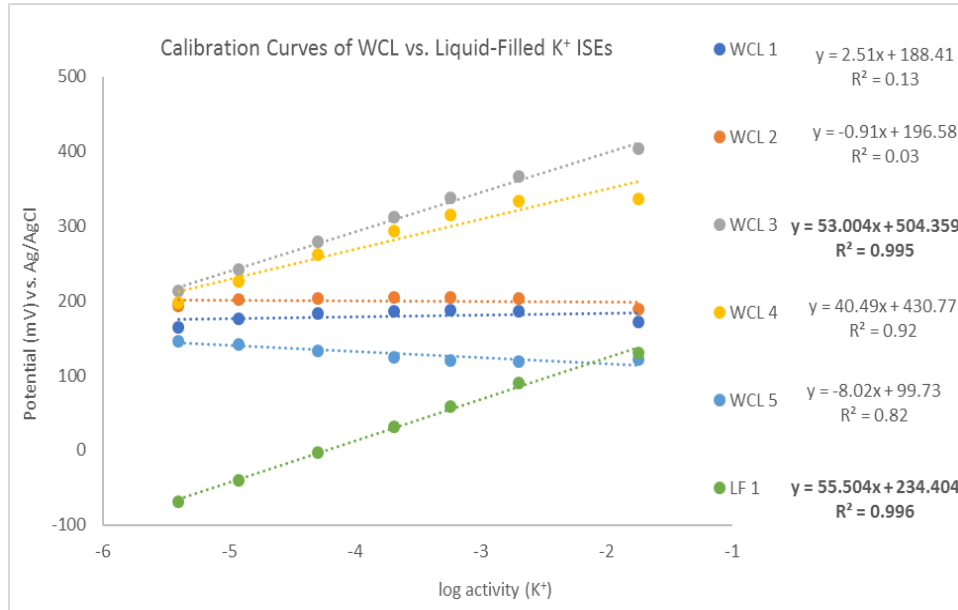


Figure 11. The calibration curves of potassium-selective WCL and LF ISEs with the same membranes in a pure KCl and water solution

The WCL-Type ISEs that were used to conduct in situ measurements on the Phoenix Lander were constructed to test their viability for the purposes of this project. One issue that was immediately realized was the difference in response compared to liquid-filled ISEs made with the same membrane components. Figure 10 includes the response curves of 5 WCL-type and 3 Liquid-filled (LF) K^+ -selective ISEs all constructed at the same time with the same membrane reagents. The expected response is an increase in potential as standard additions are added over time to the solution. The LF ISEs all behaved very similar with stable potentials. Only WCL 3 behaved this way. WCL 4 did not respond with the same increase in potential at higher concentrations. WCL 1, 2 and 5 all did not respond positively. WCL 5 did not show any characteristics of typical ISE behavior and did not respond to any calibration spikes, while WCL 1 and 2 responded to calibration spikes, but not with an ideal slope. The calibration plot (Figure 11) includes the linear fits of the response to the log of activity $_{K^+}$ for the 5 WCL ISEs and 1 of the LF ISEs. Only one LF ISE curve is presented because of the overlap between the three ISEs that would prevent clarity in the calibration plot. The LF ISEs had nearly Nernstian slopes with high R^2 values of at least 0.99. This was true for only WCL 3. WCL 4 did respond positively but with a much lower slope. WCL 1, 2 and 5 did not respond to K^+ as the LF ISEs did. Other calibrations on the same day confirmed this behavior was characteristic of the electrodes and not a one-time error (See SI Figure 36).

Because the ISEs were to be potentially deployed underwater at depths of 200 meters⁵ in the subglacial lake and up to 7 meters in the coastal pond,¹ pressure tests were performed to test the robustness of the ISEs. The pressure test included calibrations of the electrodes before and after experiencing the high pressures. The pressure was raised to about 50 atmospheres over 10 minutes with the electrodes submerged in 1 mM KCl in the chamber, maintained for 10 minutes and then slowly decreased to atmospheric conditions over 5-10 minutes. The calibrations before and after

the pressure test are shown below in Figure 12. The linear range in these plots is less than the typical K^+ -ISEs' range, but using a cation-selective rather than K^+ -selective membrane was enough to produce preliminary results. The slopes of the electrodes changed by less than 1 mV and the intercepts by less than 5 mV.

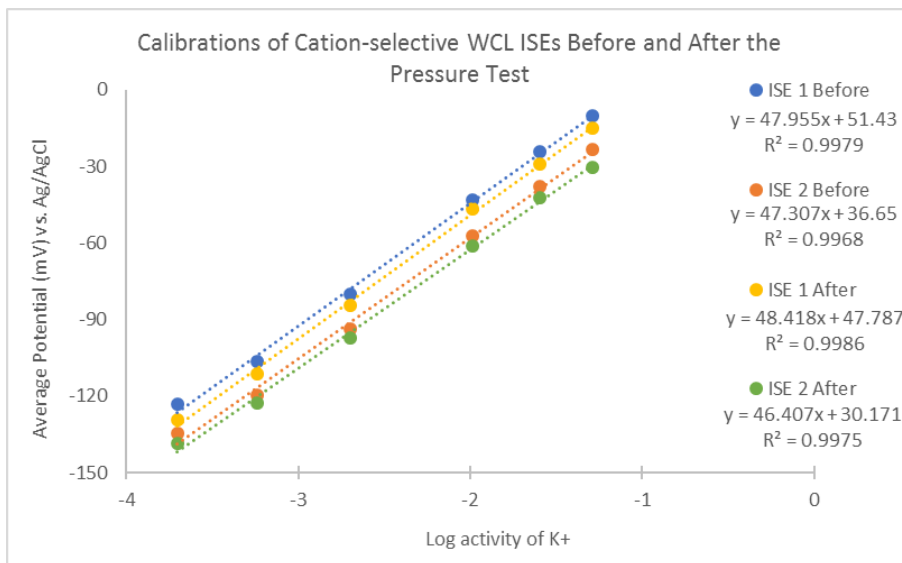


Figure 12. The calibration plot of cation-selective WCL ISEs using spikes of KCl performed immediately prior to and after exposing the electrodes to high pressures.

2d. Construction and characterization of Newly-Designed (ND) electrodes

The ND ISEs were constructed in an analogous manner to the WCL ISEs with moderate changes. To solve the performance issues of the WCL electrodes, the design and housing material were modified. Instead of the ULTEM™ polymer inner and out housings, a similar inner housing structure was constructed from Type 1 PVC, a type of housing material that was chemically resistant and guaranteed to work in the temperature range of -15 to 60°C, within the temperature range expected in the field. The ND ISEs had similar dimensions to the WCL ISEs in terms of the depth of the well for the hydrogel solution and the amount of anodized silver wire exposed to the hydrogel solution (Figure 13). The same membrane components were used as for the WCL

electrodes tested in previous experiments. The change in the housing material allowed THF, the solvent in the membrane cocktail, to dissolve the PVC and form a chemical seal to the housing. The WCL ISEs relied on the outer housing to hold the membrane in place over the hydrogel. A photograph of the ND ISEs is shown below in Figure 14. The grey housing is filled with a clear hydrogel and topped with a clear plasticized PVC membrane. At the back of the housing is a black heat-shrink covering a lead wire that was soldered to the silver wire.

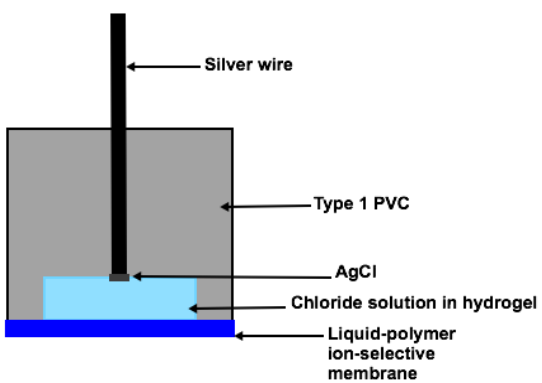


Figure 13. A schematic of the Newly Designed ISEs

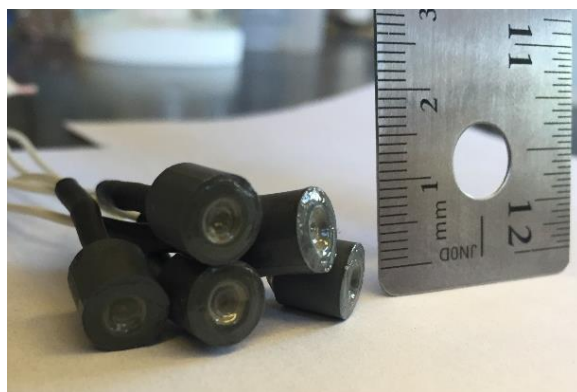


Figure 14. A photo depicting the dimensions of the ND ISEs

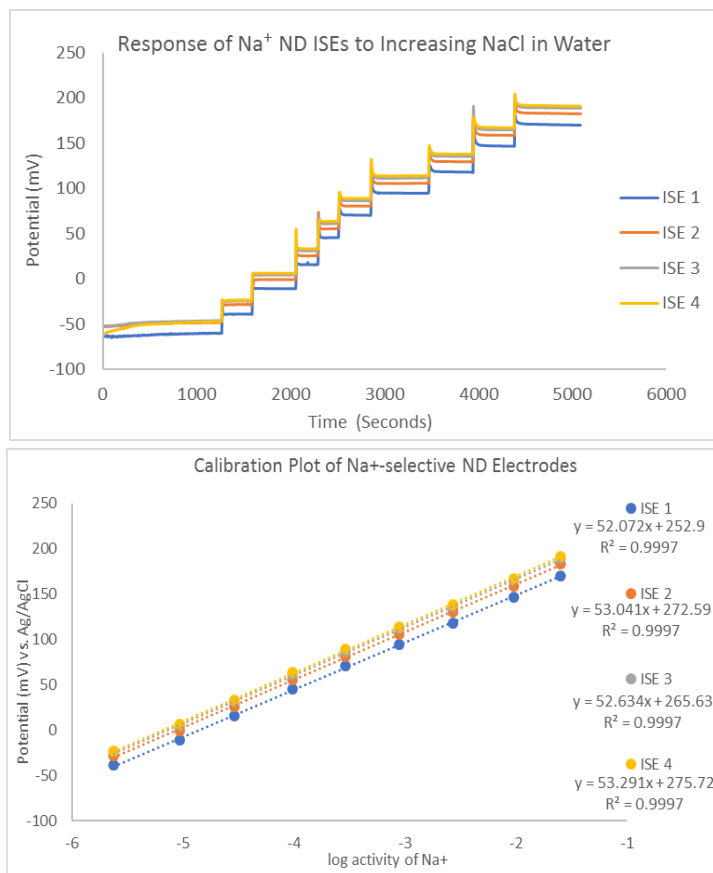


Figure 15. The response curves and calibrations of Na⁺-selective ND ISEs to spikes of NaCl in water

Figure 15 depicts the response and calibration curves of Na⁺-selective ND electrodes. These electrodes were constructed at the same time using a published membrane cocktail.²¹ As seen in Figure 15, the potential was accompanied by little to no noise across all concentrations. There was also no drift in the response as in the WCL electrodes. The calibration of the response with the log activity of Na⁺ demonstrates that the electrodes have nearly Nernstian slopes, indicating that they are sensitive to slight changes in the activity of Na⁺. Two more identical calibrations were performed in the same day with these electrodes producing nearly identical results, confirming that the ISEs continued to respond and were not deteriorating as the WCL electrodes did in previous tests.

After confirming that the ND electrodes performed sufficiently well without the same failures as the WCL ISEs, pressure tests were performed to test the robustness of the electrodes and characterize their response to exposure to environmental conditions. The Na⁺ ND ISEs in the above calibration were used in these tests. Calibrations were performed immediately before and after exposing them to high pressures. The procedure was the same as for the WCL electrodes, except the solution in the chamber was a dilute NaCl solution. The results are summarized below in Table 2. After the first pressure experiment, the ISEs experienced minor changes in their slope, retaining their sensitivity, but a large shift in the intercept occurred. With subsequent pressure tests, the effect on the intercept decreased until the intercept changed by only 5-6 mV. The results of these experiments along with the improved performance over the WCL electrodes allowed them to be tested under the various conditions expected in the environment. This method of “pressure conditioning” was incorporated as part of the construction method for the second expedition to Oyster Pond. It was not incorporated before the first expedition in July because the 7-m maximum depth of the pond was not initially expected to affect the ISEs. The results of pressure conditioning before the second expedition are discussed in Experimental Section 3e.

Table 2. The changes in calibrations before and after pressure tests on Na⁺-selective ND ISEs

		Pressure Test 1	Pressure Test 2	Pressure Test 3
ISE 1	Δ Slope (mV)	-1.34	+1.97	+0.07
	Δ Intercept (mV)	-13.1	+7.27	-5.29
ISE 2	Δ Slope (mV)	-0.45	+2.33	+0.73
	Δ Intercept (mV)	-28.6	+5.31	-6.04

3. Testing and preparation for in-situ measurements

3a. Calibrations under expected conditions – sulfidic, anoxic and mixed solutions

An array of ND ISEs used to analyze the samples included Na^+ , K^+ , Mg^{2+} , Ca^{2+} , and Cl^- ISE because these ions were expected both in Oyster Pond and the Skaftá subglacial lakes. The ISEs were calibrated with standard additions of potassium, magnesium and calcium chloride in deionized water and in background that simulated the samples. Sodium was not included in the standard addition solution for the calibrations because it was present in a high concentration in the background solution. The background solution mimicked the major ions found in the samples that were not in the standard addition solution (Table 3). Data about the samples were received through personal correspondence with Mark Skidmore, the person who collected the samples. The sensitivity of the ISEs to sulfide was tested with incremental additions of sodium sulfide to a background of equal parts KCl , MgCl_2 and CaCl_2 . The sensitivity was monitored through drift of the potential and whether the potential substantially changed upon addition of sulfide. The drift of the electrodes was measured because of drifting potentials of ammonium ISEs in response to sulfide reported in the literature.²³

The array of ND ISEs was then tested under anoxic conditions because both the Skaftá lakes and Oyster Pond have anoxic regions in the water column. Solutions were deoxygenated by bubbling ultra-high purity N_2 gas into the background solution (Table 3) for at least 30 minutes. N_2 was then continuously bubbled in the solution during calibrations. The calibration solution (Table 3) was added in increasing amounts to deionized water to calibrate the electrodes and characterize their response.

Table 3. The contents of the samples from the Skaftá Lakes and calibration solutions.

Ion	East Skaftá Sample (μM)	West Skaftá Sample (μM)	Background Solution (μM)	Skaftá Calibration Solution (M)
Li ⁺	0.0	0.0	1.0	
Na ⁺	20.1	652.7	2020.2	.012
K ⁺	1.5	52.9		.010
Mg ²⁺	2.4	10.6		.010
Ca ²⁺	3.5	111.7		.010
F ⁻	0.0	5.4		
C ₂ H ₃ O ₂ ⁻	0.0	926.3		.010
Cl ⁻	20.5	67.9		.030
Br ⁻	0.0	0.0		.001
SO ₄ ²⁻	2.0	71.4	9.0	.010
PO ₃ ²⁻	0.0	0.5		
S ₂ O ₃ ²⁻	0.0	38.1	4.2	
NO ₃ ⁻	1.7	0.0		
C ₂ O ₄ ²⁻	0.0	0.2		
S ²⁻	0.0	1009.0	1000.	

Selectivity tests were necessary to de-convolute the response of the ISEs in the mixed solutions and measure the selectivity of the electrodes for their primary ion. The interfering ion was maintained at a background concentration of 0.1 M. Then, standard additions of the primary analyte were added. This method is widely known as the Fixed Interference Method.¹⁴ The calculations were performed as described in the literature. The equation is listed below for reference. *I* is the primary ion and *J* is the interfering ion; *a* is the activity; *K* is the selectivity coefficient for ion I in the presence of ion J.¹⁴

$$E = E^{\circ} + \frac{59.18 \text{ mV}}{z} \log a_I + K_{IJ} a_J \quad (\text{Equation X})$$

3b. Analysis of real samples - Skaftá subglacial lakes

Samples from the West and East Skaftá lakes were used to test the electrodes' ability to respond to a real sample rather than a simulated environment. The samples were kept at 4°C in sealed polyethylene bottles after they arrived from Mark Skidmore (Montana State Univ.) Upon

completion of these tests and calibrations described prior, the ion content of Skaftá samples was measured with the tested array of ND ISEs which included ISEs selective for K^+ , Na^+ , Mg^{2+} , and Ca^{2+} , the major ions expected in the samples and in Oyster Pond. The ISEs were left in the sample until they reached a stable potential and remained at that potential for at least 20 minutes. An Orion™ conductivity probe (Thermo Scientific) was then used to measure the ionic strength of the samples in order to convert the activities of the ions to concentrations (Supplemental, Figure 37).¹³ The calibrations of the ISEs before and after measuring each sample using the background solution and calibration solution (Table 3) are also listed in the supplemental section in Table 15. These calibrations were used to calculate the concentrations of each ion in the samples.

3c. Tests of array and commercial sulfide electrode in seawater simulants

The content of the calibration solutions mimicked the ratios of the major ions in seawater (Table 4). Serial dilutions of the calibration solution resulted in a total of 6 decreasingly saline solutions, the most dilute containing 1.2×10^{-5} M Na^+ . Ammonium and nitrate are not typically present in seawater but were included in the calibration solution because it is possible that Oyster Pond is nitrogen-enriched due to runoff and septic leakage.¹ All electrodes in the array were calibrated with these solutions both in the lab and in the field. Approximately 100 mL of the proper calibration solution was poured into a plastic 250-mL beaker. The beaker was held underneath the array with the membranes of the electrodes submerged for about 5 minutes (Figure 17). The software was started after submerging the electrodes. When switching between calibration solutions, data collection was paused and then resumed immediately after re-submerging the electrodes to avoid excessive electrical noise when the electrodes were not in an aqueous solution. To avoid contamination between solutions, the calibration was done in order of increasing salinity.

The final calibrations in seawater solutions were performed using the Deep-Sea Lawson Box as the potentiometer to test the field instrumentation, described in Experimental Section 4a.

Table 4. The concentrations of ions in seawater and in the ISE array calibration solution.

Ion	Seawater¹⁵ (mol/L)	Seawater Calibration Solution (mol/L)
Na ⁺	0.459	1.202
Mg ²⁺	0.052	0.010
Ca ²⁺	0.010	0.010
K ⁺	0.010	0.001
*NH ₄ ⁺	----	0.010
Cl ⁻	0.535	1.220
SO ₄ ²⁻	0.028	0.100
HCO ₃ ⁻ /CO ₃ ²⁻	0.002	0.001
*NO ₃ ⁻	----	0.010

The response the sulfide electrode (Orion™, Ag⁺/S²⁻ electrode) was characterized in a sodium chloride solution and a seawater simulant solution to calibrate the electrode for the conditions expected in the pond. Standard Na₂S solutions were prepared from Na₂S·9H₂O (Sigma-Aldrich) that was saturated in deionized, de-aerated water and then diluted. The solutions were standardized by titrations with Pb(ClO₄)₂ using the sulfide electrode as the endpoint indicator. This procedure was modified from the manufacturer's instructions by not adding an anti-oxidant buffer to the standards or sample solutions because it would not be possible to add such a buffer when making in-situ measurements with the sulfide electrode. The standard solutions were used within three days to avoid loss of sulfide. The electrode was first calibrated in deionized water with standard additions of the standard Na₂S solution. It was then calibrated in a background of NaCl with the same standard additions of Na₂S. Then the electrode was calibrated in a 1:10 dilution of the seawater calibration solution (Table 4) as the background.

3d. Temperature probe test

The submersible temperature probe (HOBO® Water Temp Pro v2) was also tested in the laboratory before deployment in the field. The probe was submerged in water in an 800-mL beaker. Warm tap water was added to the beaker until it reached a stable temperature. In Figure 16, the temperature probe reported an

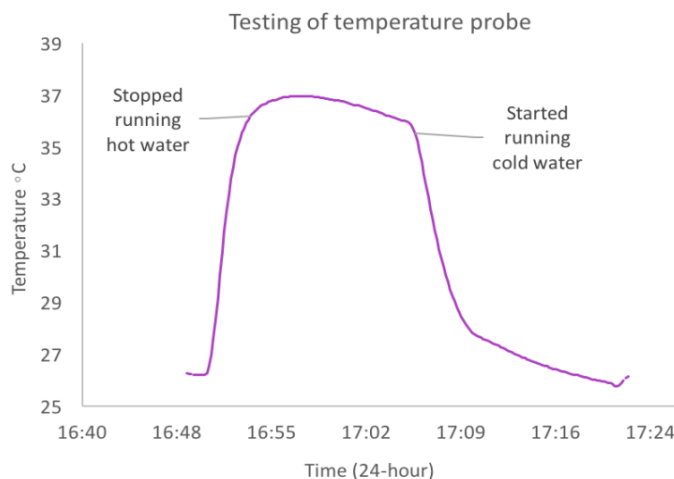


Figure 16. Testing the temperature probe in the lab

increasing and then stable temperature of 37°C. The probe was then left in the beaker for about 10 minutes without adding any hot water. Then cold water was run into the beaker as indicated by the probe with a decrease in temperature to about 26°C. This test indicated that the probe had a short response time of a few minutes and was responding appropriately to changes in temperature. A second thermometer was not used to confirm the accuracy of the temperature reading, because only relative changes in temperature were needed to convert the response of the ISEs from the temperature at depth to its response at the calibration temperature. A second thermometer would also not be available during field measurements.

3e. Pressure conditioning

Results of the first expedition demonstrated the need to condition the electrodes in preparation for a high-pressure environment. Pressure tests were performed similarly to previous experiments. All the ISEs, except for the sulfide electrode, were submerged in deionized water in the pressure chamber. The pressure tests were performed three times with calibrations before and

after each test (Table 5). The purpose of the pressure tests was to “pressure condition” the electrodes by exposing them to pressures much higher than those expected in the deepest parts of the pond. This process ensures that any compression or shifting of the internal components of the electrodes occurs prior to field deployment and not during the in-situ measurements as had likely occurred during the first field expedition. The electrodes that changed the least upon exposure to pressure for the second and third times (in bold) were chosen for the field array.

Table 5. The changes in the calibrations of the ND ISEs after pressure conditioning

ISE Name	After Pressure Test 1		After Pressure Test 2		After Pressure Test 3	
	Δ Slope (mV)	Δ Intercept (mV)	Δ Slope (mV)	Δ Intercept (mV)	Δ Slope (mV)	Δ Intercept (mV)
Mg 1	9.2	29.3	-0.1	-12.2	-2.2	-16.0
Mg 2	8.8	26.2	0.0	-1.8	-1.4	-15.9
Mg 3	8.5	31.4	0.4	-1.6	-2.8	-25.8
Mg 4	7.2	18.8	-1.7	-10.7	-0.3	-2.4
Ca 1	3.6	24.0	0.8	9.0	3.6	23.3
Ca 2	3.6	22.7	3.4	4.9	0.8	17.8
Ca 3	4.4	23.0	2.0	9.4	1.5	21.8
Ca 4	5.6	21.8	0.4	5.7	2.2	16.1
NH ₄ 1	--	--	1.1	5.2	2.4	9.0
NH₄ 2	--	--	1.1	4.8	-0.4	-6.0
NH₄ 3	6.6	13.3	1.0	6.1	1.4	6.7
NH ₄ 4	5.0	17.0	2.0	2.9	0.7	11.5
Na 1	3.8	11.6	0.9	3.3	2.7	2.1
Na 2	4.5	9.7	-0.3	1.4	2.5	5.2
Na 3	4.0	8.9	-0.9	0.4	3.0	4.9
Na 4	4.5	9.4	-2.8	4.4	5.0	-0.7
Cl 1	8.0	-6.9	2.8	-51.5	-3.3	32.0
Cl 2	8.9	-27.3	1.1	5.5	-1.1	-32.1
Cl 3	5.8	-47.2	0.7	-17.1	-1.4	45.2
Cl 4	7.7	-8.3	0.9	-1.3	-2.2	-2.4
NO ₃ 1	0.9	-7.4	-8.1	-17.0	6.3	-13.8
NO ₃ 2	--	--	-7.5	-12.9	5.7	-20.1
NO₃ 3	0.4	-11.5	-7.1	-15.0	4.4	-19.6
NO₃ 4	0.8	-5.3	-6.2	-9.7	5.9	-11.1

4. In-situ measurements at Oyster Pond

4a. Instrumentation and electronics

The potentiometer used to measure the potentials reported by the electrodes was a modified EMF16 (Lawson Labs, Inc.). The typical EMF16 was removed from its standard chassis and put into a waterproof aluminum chassis with waterproof input and output plugs (SEACON). The potentiometer was powered by a 12 V rechargeable battery pack instead of an AC source during field measurements. Connections between the SEACON plugs and the electrodes were manually soldered and waterproofed with heat-shrink and Plasti-Dip®. The potentiometer was bolted to a steel cage



Figure 17 . The experimental setup including the modified potentiometer in a waterproof aluminum chassis and array of electrodes during field calibrations

during field deployment (Figure 17). The signal from the potentiometer was sent to a Toughbook laptop through a load-bearing, waterproof cable (SEACON) and analyzed with software provided by Lawson Labs, Inc. When calibrating on the dock or in the lab, it was necessary to ground the chassis to the solution with a wire and platinum working electrode (PalmSens, 2 mm diameter, PTFE coating). This was not necessary during in-situ measurements because the chassis was in direct contact with the pond water.

Because the electronics, electrodes and supporting steel cage weighed over 20 kg, it was necessary to create a support system for safely raising and lowering the array in the water column. A pulley and locking hand-winch were bolted to a plank of wood that was then tied to a heavy

duty inner tube (Figure 18). The rope used to support the steel cage was 500-pound grade parachute cord. The advantages of this system are the ability to lock the hand-winch in place when the desired depth was reached and the complete support of weight by the inner tube rather than by the boat.



Figure 18 . The inner tube and pulley system that supported the cage, electronics and electrodes during in-situ measurements

4b. Field site description, in-situ data collection, and sampling

Expeditions to Oyster Pond occurred on July 29th, 2016 and August 28th, 2016. The two sampling sites in Oyster Pond, marked in red in Figure 19, are in the two main basins of the pond. Both sampling sites were at permanently anchored buoys managed by OPET. The buoy in the northern, upper basin is named OP1 and the buoy in the southern, lower basin is named OP3.²⁴ During the first expedition, a calibration of the array of electrodes was performed before in-situ measurements and batch sampling at OP3. Due to time constraints, it was not possible to sample at OP1 or to perform a calibration after the in-situ measurements were complete. In August, a 6-point calibration was performed on the dock both before and after taking field measurements. In-situ measurements and batch sampling were performed first at OP3 and then at OP1 before returning to the dock to recalibrate the electrodes.

At each sampling site, the electrodes were first allowed to stabilize at the water surface. Then the array was lowered in 0.2 to 0.5 meter intervals and allowed to stabilize at least 5 minutes at each depth. The bottom, or sediment-water interface, was assumed to be the depth at which large

bubbles surfaced due to the steel cage disturbing the sediment. Any further lowering of the cage cause some slack in the rope and cable. After the electrodes stabilized at the bottom of the pond, the array was brought up to the surface over a few minutes without pausing. The electrodes were then allowed to re-stabilize at the surface (0.3 meters deep). During re-stabilization at the surface, batch samples were collected from the other side of the boat to not expose the array of ISEs to water brought up from below.

The temperature was recorded using an underwater data logger (HOBO® Water Temp Pro v2) both during the field calibrations and the in-situ measurements. It was set to a logging interval of 10 seconds. For the in-situ measurements, the probe was

attached to the steel cage at the same depth as the array of electrodes to ensure that the ISE measurements could be correlated with the temperature measurements. As shown in Experimental Section 3d, the probe took about 2-3 minutes to respond, so the temperature was averaged for each calibration point and each depth after excluding the first 3 minutes to allow for it to fully respond.

Depth in the water column was recorded by marking the rope with permanent marker at each depth the electrodes were allowed to stabilize at. Because parachute cord stretches, the stretch in the cord was simulated by applying 15-20 kg of tension to the cord on land to measure the



Figure 19. A topographical map of Oyster Pond and the sampling sites (Modified from Emery et al.)

change in length. The ratio of stretched to relaxed rope was applied to all the depth markings made on the rope.

Batch samples were collected at 0.5 to 1 meter intervals using a Fieldmaster® water sampler with a volume of 1.75L (Figure 20). The sampler was lowered into the water with the longer side horizontal to the surface which allowed for collection of a sample at depth with an uncertainty of a few centimeters. After bringing the sample to the surface, it was poured in a



Figure 20. Fieldmaster® Water Sampler

sterile Whirl-pak® bag and sealed. Within a few hours, the samples were refrigerated until further analysis in the lab. During the first expedition, samples were only collected at OP3. During the second expedition, samples were collected at both OP1 and OP3.

5. In-lab analysis of Oyster Pond samples

5a. Conductivity and pH

The samples were removed from the fridge and allowed to come to room temperature. Sterile, 25-mm Nalgene filters with surfactant-free, cellulose acetate 0.22- μ m membranes (Thermo Scientific) and sterile, 5-mL Luer-Lok™ syringes (BD Syringe) were used to filter about 50-mL of each sample into clean, 20-mL plastic scintillation vials, producing two replicate filtered aliquots of each sample.

An Orion™ Conductivity Probe (Thermo Scientific) was first calibrated using the manufacturer's standards containing pure NaCl. It was then calibrated (Figure 21) using the ICP standards that had NaCl in a concentration about 10 times greater than that of the other main

constituents of seawater, as was expected in the Oyster Pond samples (Table 6). A glass combination pH electrode (Sensorex) was calibrated using buffers of pH 4.00 to 10.00 (Fisher). The calibrated conductivity and pH probes were then used to collect data from each sample with thorough rinsing and drying of the electrodes between samples. There were two replicate vials of each filtered sample.

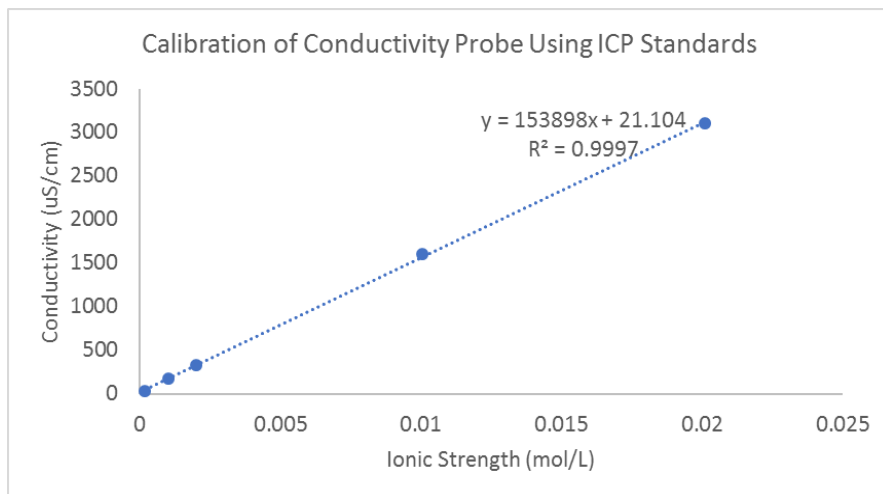


Figure 21. The calibration of the conductivity probe using the known ionic strength of the ICP standards

5b. ICP-AES

Standards for analysis by inductively couple plasma atomic emission spectroscopy (Leeman Labs PS-1000) were made using deionized water (18.2 MΩ) and chloride salts of sodium, magnesium, calcium and potassium. A small amount of sodium sulfate was also used to mimic the sulfate content of seawater.^{15,25} The goal was to prepare standards that mimicked the content of seawater in that NaCl was the main component at a 10 times higher concentration than the other salts. The concentrations of the standards are shown below, along with the calibration curves produced for the instrument (Table 6, Figure 22). The samples were diluted by 10 using deionized water to keep the range of concentrations within the limits of the calibration curves. Six total replicates of each sample were used, 3 replicates from each vial of filtered sample.

Table 6. The contents of the ICP standards for Oyster Pond sample analysis

Standard	Sodium (mg/L)	Magnesium (mg/L)	Calcium (mg/L)	Potassium (mg/L)	Chloride (mg/L)	Sulfate (mg/L)	Uncertainty (mg/L)
1	447	26	68	39	275	74	1
2	224	13	34	19	138	37	1
3	44.7	2.6	6.8	3.9	27.5	7.4	0.1
4	22.4	1.3	3.4	1.9	13.8	3.7	0.1
5	4.47	0.26	0.68	0.39	2.75	0.74	0.05

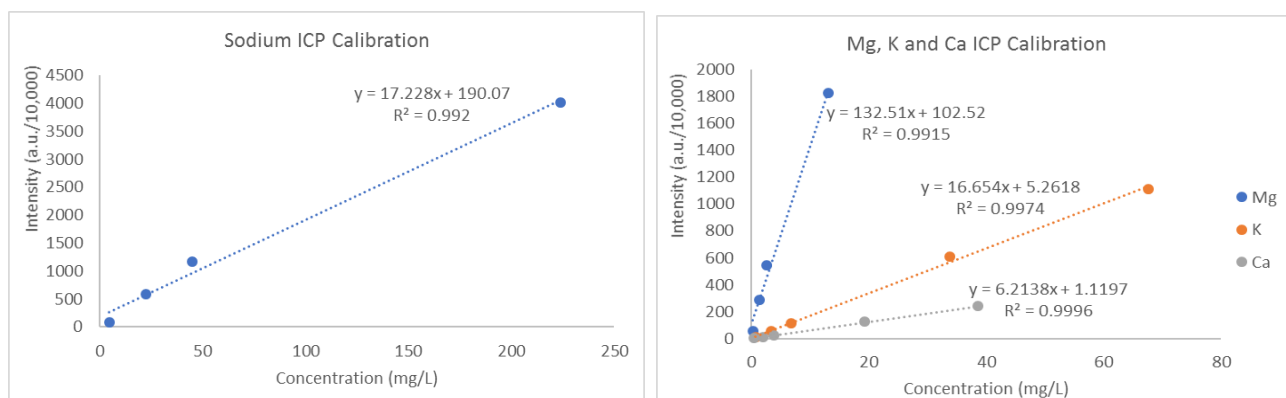


Figure 22. The calibration plots for the response of the ICP-AES to the prepared standards

5c. Ion chromatography (IC)

The standards for the calibration of the Dionex Ion Chromatography System-2000 were the Six Cation Standard (Number II, Dionex) and the Seven Anion Standard (Number I, Dionex). These standards were diluted as shown below in Table 7 and Table 8 to produce a 4-point calibration curve for cations and 3-point calibration for anions. Custom standards were not made because matrix issues should not have affected these results due to the separation of ions. To prevent column overloading, samples were diluted by 50. Three replicates of each sample were used in this analysis. Because the analysis took about 3 days using a method that ran each standard and sample for 30 minutes, a calibration was run every 24 hours. The samples and standards were all prepared at the same time, frozen at -20°C , and thawed just prior to loading the autosampler every 24 hours, ensuring that the samples and standards were treated in the same way while

preventing significant evaporation. The linear regressions for the calibration of all ions had R^2 values greater than 0.99 (not shown).

Table 7. Concentrations of the cation IC standards prepared from the Dionex stock

Cation	Stock (mg/L)	Standard 1 (mg/L)	Standard 2 (mg/L)	Standard 3 (mg/L)	Standard 4 (mg/L)
Li⁺	49.7	4.97	0.249	0.00497	0.00020
Na⁺	199	19.9	0.995	0.0199	0.00080
NH₄⁺	248	24.8	1.24	0.0248	0.0010
K⁺	499	49.9	2.50	0.0499	0.0020
Mg²⁺	249	24.9	1.25	0.0249	0.0010
Ca²⁺	498	49.8	2.49	0.0498	0.0020

Table 8. Concentrations of the anion IC standards prepared from the Dionex stock

Anion	Stock (mg/L)	Standard 1 (mg/L)	Standard 2 (mg/L)	Standard 3 (mg/L)
F⁻	20.1	1.01	0.050	0.0050
Cl⁻	29.7	1.49	0.074	0.0074
NO₂⁻	101	5.05	0.253	0.0253
Br⁻	99.3	4.97	0.248	0.0248
NO₃⁻	99.7	4.99	0.249	0.0249
PO₄³⁻	151	7.55	0.378	0.0378
SO₄²⁻	151	7.55	0.378	0.0378

Results

1. Preparation and testing for in-situ measurements

1a. Calibrations under expected conditions – sulfidic and anoxic

In the subglacial lakes and at Oyster Pond, the ions to be measured with ISEs were Na^+ , K^+ , Mg^{2+} , Ca^{2+} , NH_4^+ , and Cl^- , major constituents of the subglacial lakes⁶ and the seawater that feeds coastal ponds.¹⁵ Electrodes selected for these ions were incorporated into an array and tested under expected environmental conditions such as sulfidic and anoxic solutions, as well as complex matrices of the many ions found in natural waters. In Table 9, calibrations of Mg^{2+} , Ca^{2+} and Cl^- ND ISEs are shown. Chloride salts of magnesium, calcium and potassium were added to deionized water. The Mg^{2+} and Ca^{2+} ISEs had nearly Nernstian slopes over a wide working range of 0.5 μM to 1 mM in water. Higher concentrations were not tested in this experiment. The Cl^- electrodes were not as sensitive as an ideally-behaving ISE and had slopes of -27 to -35 mV per decade of activity in this range.

After it was confirmed that the electrodes calibrated properly, they were tested under sulfidic conditions. The same spikes of solution were added as in the calibration in water, but the background solution was about 1 mM H_2S , or 30 ppm, at pH 5.3 buffered with acetic acid. The results are compared to calibrations in water (Table 9). The Mg^{2+} and Ca^{2+} ISEs were not affected much by the sulfide background. The Cl^- ISEs did not have a negative slope, and their behavior was not linear or characteristic of an ISE.

Table 9. Comparison of the calibration of ND ISEs in water and in a sulfidic solution.

ISE Type	Calibration in Water <i>Slope and intercept in mV</i>	Calibration in Sulfide <i>Slope and intercept in mV</i>
Mg²⁺	$y = 23.9x + 123$ $R^2 = 0.996$	$y = 22.5x + 117$ $R^2 = 0.981$
Ca²⁺	$y = 24.5x + 170$ $R^2 = 0.985$	$y = 20.3x + 122$ $R^2 = 0.966$
Cl⁻	$y = -35.3x + 71$ $R^2 = 0.991$	$y = 3.0x + 166$ $R^2 = 0.368$

Note: y is the measured potential, E , and x is the log of the activity.

Two more sulfide exposure tests were then performed on these electrodes. First, the ISEs were placed in background of 0.1 mM MgCl₂, CaCl₂ and KCl, and then spikes of the sulfide solution were added. Then, the drift of the electrodes was compared between a 0.1 mM MgCl₂, CaCl₂ and KCl background and the same salt background with the addition of the sulfide solution at a concentration of 0.1 mM (Figure 23a-c). In Figure 23a, the concentration of sulfide was calculated using the response of the Na⁺ ND ISE to Na₂S. The calibration of this ISE is shown in Supplemental Figure 38. The increasing sulfide concentrations did not have a significant effect on any of the other cation ISEs. It did, however, cause a change in the response of the Cl⁻ ISEs. It is also important to note that the Cl⁻ ISEs became inconsistent with each other. In the drift tests, the cation ISEs did not demonstrate a significant difference between a 0.1 mM chloride salt background and the 0.1 mM chloride salt + sulfide background. The chloride ISEs did not drift more over the entire analysis period, but it is clear that the potential decreased and then increased, rather than remaining stable like the potential of the Ca²⁺ and Mg²⁺ ISEs. These results demonstrate the lack of an effect of sulfide on the cation-selective ND electrodes and the substantial influence sulfide has on the response of the Cl⁻ ISEs.

Because anoxic conditions were expected in both the subglacial lakes and at Oyster Pond, tests were conducted in oxic and anoxic conditions to determine if there was an effect on the

behavior of the ND ISEs. Anoxic solutions were made from deionized water degassed with ultra-high purity N₂ gas before and during the calibration. The ISEs were calibrated using additions of a mixed salt solution of NaCl, MgCl₂, CaCl₂ and KCl. The response curves are shown in SI Figure X, and the calibrations are summarized in Table X, below. None of the ISEs demonstrated any significant difference in behavior from concentrations of 10⁻⁶ to 10⁻² M. The largest change in the intercept was 10 mV, but this change in the intercept is typical in between normal calibrations.

Table 10. Comparison of the calibrations of ND ISEs in oxygenated and anoxic conditions.

ISE Type	Oxic Conditions <i>Slope and intercept in mV</i>	Anoxic Conditions <i>Slope and intercept in mV</i>
Na⁺	$y = 52.0x + 274$	$y = 54.6x + 284$
K⁺	$y = 44.3x + 208$	$y = 47.4x + 219$
Mg²⁺	$y = 23.4x + 106$	$y = 22.9x + 108$
Ca²⁺	$y = 22.9x + 130$	$y = 23.1x + 134$

Note: y is the measured potential, E, and x is the log of the activity.

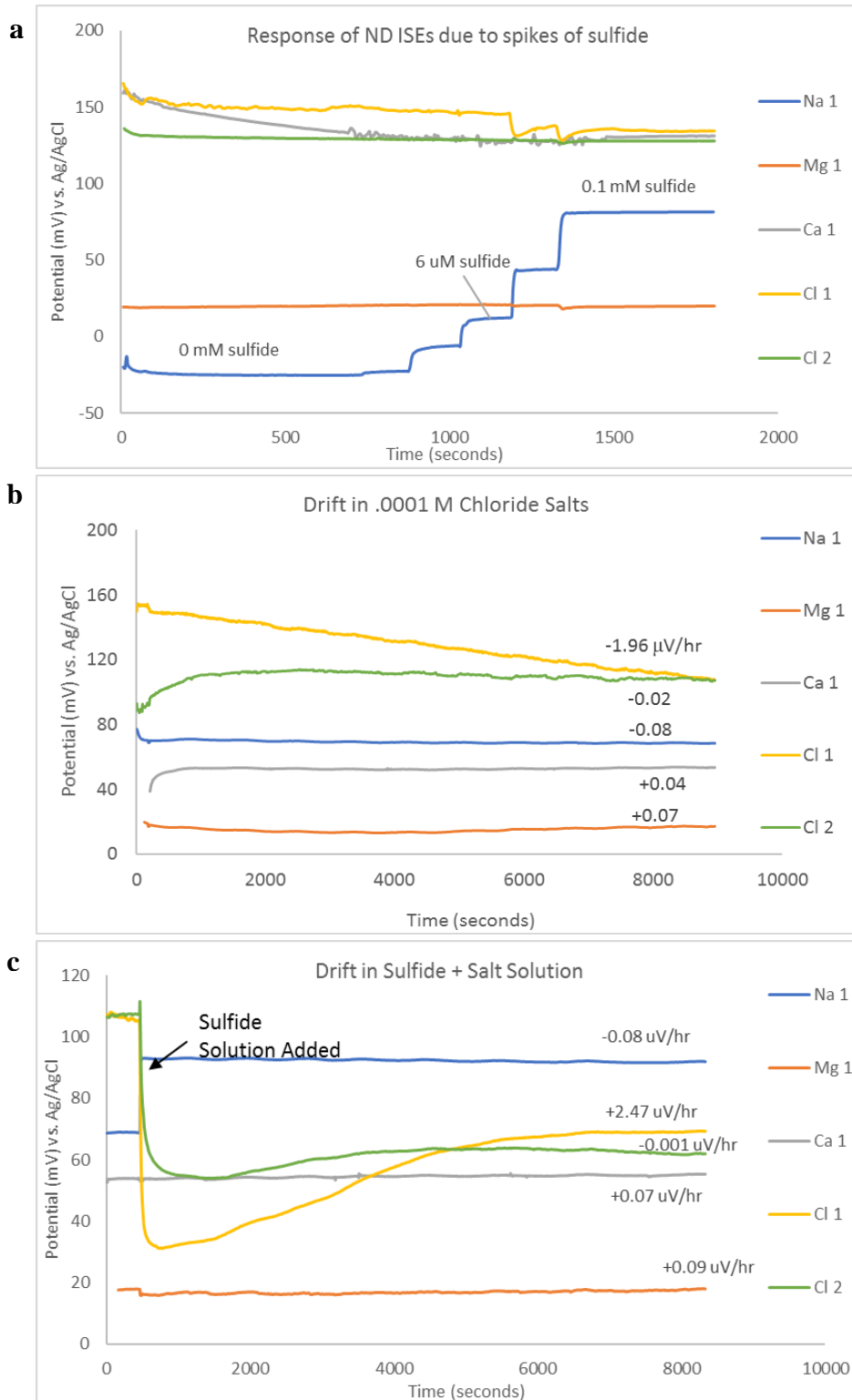


Figure 23. The effects of sulfide on the ND ISEs

Figure (a): Response of the ND ISEs to increasing sodium sulfide concentrations with an initial solution concentration of $0 \mu\text{M}$ sulfide and 0.1 mM MgCl_2 , CaCl_2 and KCl . Figure (b): Drift of the ND ISEs over time in a 0.1 mM solution of MgCl_2 , CaCl_2 and KCl . Figure (c) shows the drift of these same ISEs in a solution of 0.1 mM MgCl_2 , CaCl_2 and KCl and 0.1 mM sulfide. The black arrow marks when the sulfide was added to this solution. The drift was averaged from 2000 to 8000 seconds in b and c.

Ib. Analysis of real samples - Skaftá subglacial lakes

The next test of the electrodes' performance was to observe their response in a real sample. Samples from the West and East Skaftá lakes were received from Mark Skidmore (Montana State University). The range of concentrations in the calibration was from μM to mM , as was expected in the samples from Mark's data. The calibrations are listed in Supplement Table 15, and were performed using the described background and calibration solutions in Table 3. The calibrations before and after each sample were averaged to calculate the concentrations of analyte. These samples were also analyzed by ion chromatography. The summary of the results of these results are listed in Table 11. The ISEs seemed to have accurately measured the amount of Na^+ based on Mark's data.

The other cation ISEs overestimated the concentration of their primary analytes, but in general they agreed with the trend that the East lake sample was more concentrated than the West lake.

Table 11. The comparison of the Skaftá sample compositions based on different analysis methods.

Ion	West Skaftá Lake			East Skaftá Lake		
	IC (μM)	Mark's data (μM)	ISEs (μM)	IC (μM)	Mark's data (μM)	ISEs (μM)
lithium	0	0.0		0.0	0.0	
sodium	5.4	20.1	18 ± 2	131.3	652.7	580 ± 110
potassium	0	1.5	53 ± 5	4.0	52.9	380 ± 20
magnesium	0	2.4	14 ± 6	5.0	10.6	6500 ± 500
calcium	1	3.5	73 ± 13	20.7	111.7	590 ± 80
fluoride	1.5	0.0		2.3	5.4	
acetate	0.5	0.0		10.7	926.3	
chloride	2.8	20.5		9.0	67.9	
bromide	1.3	0.0		1.3	0.0	
sulfate	0	2.0		11.0	71.4	
phosphate	0	0.0		1.9	0.5	

IC stands for ion chromatography measurements performed in the Kounaves Lab by a graduate student, Elizabeth Oberlin. The ISE analysis includes the selectivity coefficients of the ISEs that are shown in later results below.

Ic. Tests of array and commercial sulfide electrode in seawater simulants

Because of the mixed response that seemed to occur in some the cation-selective ISEs in the Skaftá sample analysis and the response of the Cl^- ISE to other anions, experiments were performed to calculate selectivity coefficients of the ISEs before testing them in mixed solutions mimicking the contents of seawater, a known source of water in Oyster Pond.¹ The constructed ISEs were ND-type and the method used for the experiments was the Fixed Interference Method, as described in the Experimental Section, with a background concentration of 0.1 M of the

interfering ion. In this array of electrodes tested, K^+ was not included because of its low slopes (less than 50 mV) observed in the Skaftá sample experiments, and NH_4^+ and NO_3^- ISEs were included because of possible nitrogen enrichment in the pond. Nitrate ISEs were simply an anion-selective membrane with no ionophore, so that it would respond based on the Hofmeister Series of lipophilicity,¹² as described in the methods section. The results of these experiments are summarized in Table 12, as averaged for 3 ISEs of each type. A value of -3 for $\log K_{IJ}$ is equivalent to that ISE being 1000 times more selective for the primary ion than the interfering ion. Correspondingly, -2 represents an ISE that is 100 times more selective for its primary ion in the presence of the interfering ion. The cation ISEs were generally more selective than the anion ISEs. The Na^+ ISEs were the most selective against all other interfering ions tested. The NH_4^+ ISEs were also very selective for their target ion.

Table 12. Selectivity coefficients in the form of $\log K_{IJ}$ found using the Fixed Interference Method

Interfering Ion	Na^+ ISEs	Mg^{2+} ISEs	Ca^{2+} ISEs	NH_4^+ ISEs	Cl^- ISEs	NO_3^- ISEs
Na^+	---	-5.0	-2.9	-3.0	---	---
K^+	-2.7	-4.4	0	-1.0	---	---
Mg^{2+}	-4.8	---	-3.7	-4.7	---	---
Ca^{2+}	-4.8	-1.7	---	-4.8	---	---
NH_4^+	-4.3	-4.5	-1.0	---	---	---
Cl^-	---	---	---	---	---	-2.0
NO_3^-	---	---	---	---	-1.4	---
CO_3^{2-}	---	---	---	---	-1.3	-2.9
SO_4^{2-}	---	---	---	---	-3.1	-2.5

After performing selectivity experiments, an array of 14 ISEs, 2 of each of the ND ISEs in Table X plus an extra Na⁺ ISE and a commercial S²⁻ ISE, was assembled. This array was calibrated using a solution that mimicked the contents of seawater (Table 4). As is known for seawater, NaCl was in a concentration about 10 times greater than the other ions.¹⁵ To mimic the calibration in the field as well as possible, the array was set up using the Deep-Sea Lawson Box as the potentiometer. The ISEs responded with little noise and had stable potentials throughout the calibration. The working range of the electrodes was from 1 μM to 1 M for the Na⁺ ISEs, 0.1 μM to .01 M for NH₄⁺, Mg²⁺ and Ca²⁺, and 1 μM to 1 M for the anion-selective electrodes. It is important to note that there was no sulfide in this calibration solution, although the sulfide electrode did respond. It was most likely responding to chloride as discussed later. The response time for all ISEs was fast, at less than a minute in all cases, as was desired for field-ready in-situ electrodes.

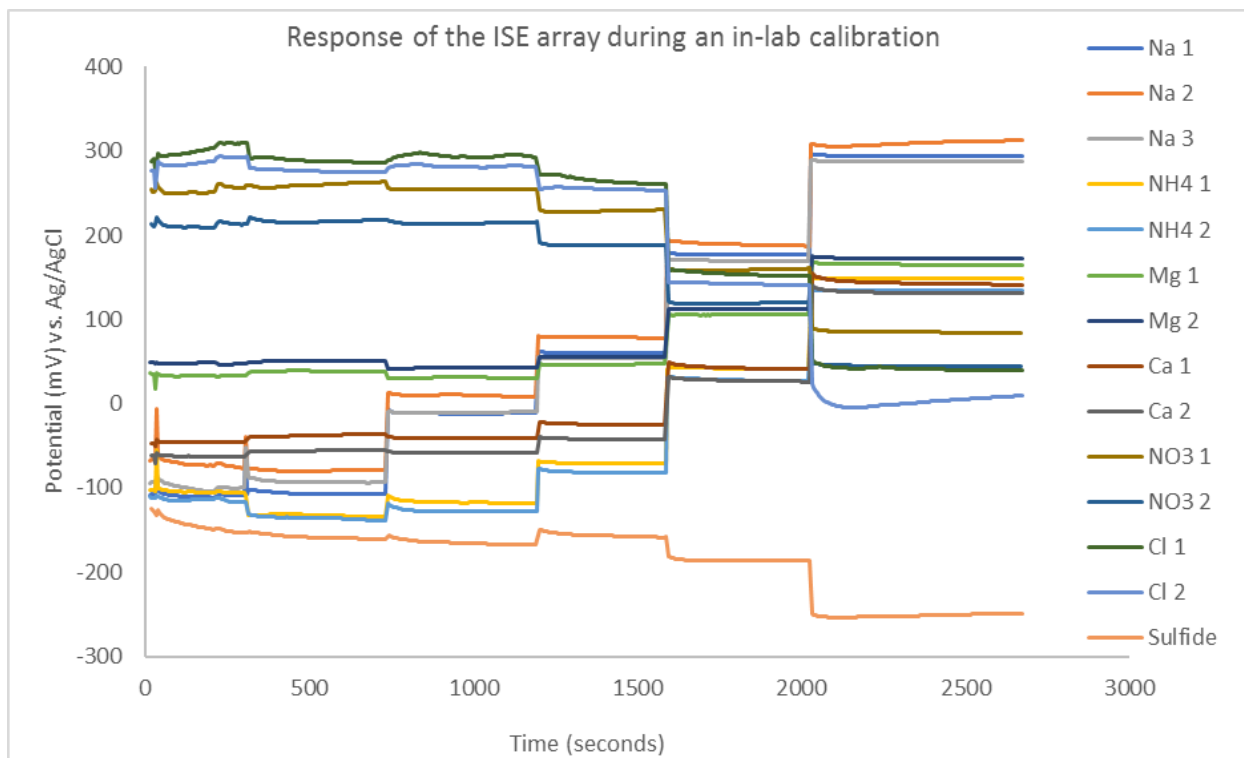


Figure 24. The response during calibration of the array of ND ISEs prepared for fieldwork in Oyster Pond using seawater simulants.

2. In-situ measurements at Oyster Pond

2a. First expedition: July 29th, 2016

Before the in-situ measurements, the array of electrodes was calibrated on the dock. The average temperature during this calibration was 27.1 ± 0.3 °C (Supplemental Figure 39). The response of the electrodes is shown below in Figure 25. Standards were used in order of most dilute to most concentrated. The potential of the electrodes was stable throughout the calibration with the exception of the drifting NH₄ #1 ISE. The potential of the cation electrodes increased with increasing concentration of the standards. The anion ISEs also performed as expected and experienced a decrease in their potential as the concentration increased. There was no sulfide in the standards, so the decrease in potential of the sulfide electrode was not due to increasing sulfide. The calibration curve for the Na⁺ ISEs is shown in Figure 25. The slopes were close to the Nernstian slope of 59 mV/z per decade of activity. Similar calibration curves for the other types of ISEs are shown in Supplemental Figure 40. The R² value was greater than 0.99 for all ISEs except the Cl⁻ ISEs that had R² values of 0.98.

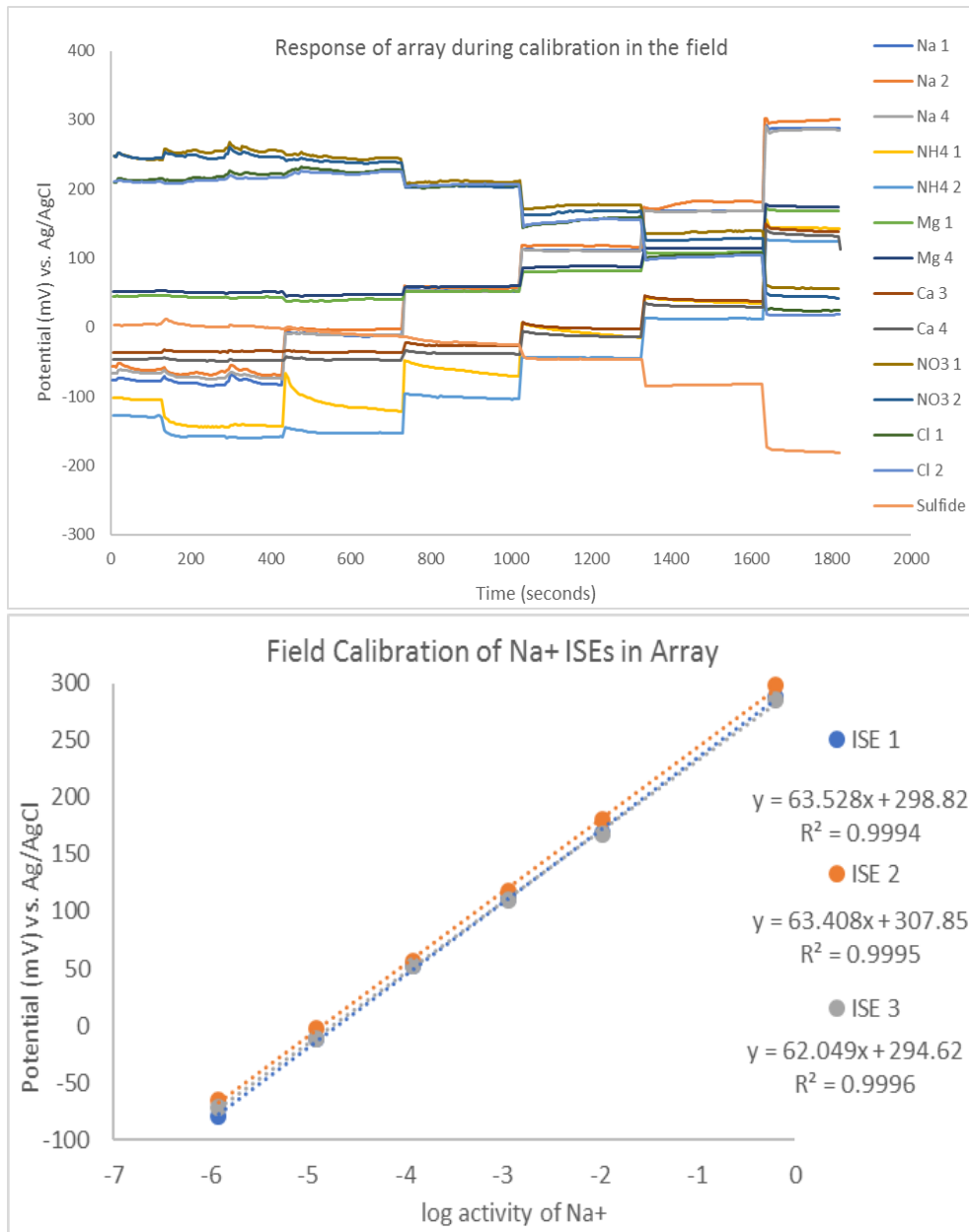


Figure 25. The response curve and calibration plot of the ND ISEs during calibration on the dock on July 29th, 2016.

The response of the array during in-situ measurements at the OP3 sampling site is shown in Figure X. At the start of data collection, the array was at the surface. The array was then periodically lowered until it reached the bottom at about 3000 seconds. After equilibrating at the bottom, the array was brought back to the surface. The “shift” labeled in the figure was not

associated with a lowering event. This potential shift was unexpected, and because it happened to all the electrodes, it may have been a shift in the electronics or in the reference electrode. At various times throughout the measurement, an ISE experienced a permanent shift in potential. For example, the ISE named NO_3^- #2 suddenly dropped in potential and became noisy after 500 seconds. This is also true for the NH_4^+ #1 ISE in yellow that became extremely noisy and unresponsive. The ISEs that did not “break” did increase in potential with depth if they were cation ISEs and decrease in potential with depth if they were anion ISEs. The fact that they did not return to the same potential at the surface means that they do not have the same response characteristics as when they were first calibrated. Unfortunately, there was not enough time to perform another calibration after collecting in-situ data because the sun was setting. The sulfide electrode had a much larger decrease in potential than during the field calibration. This occurred because of the presence of sulfide at the bottom of the pond. As discussed earlier, the sulfide electrode slightly responded to chloride in the calibration solution.

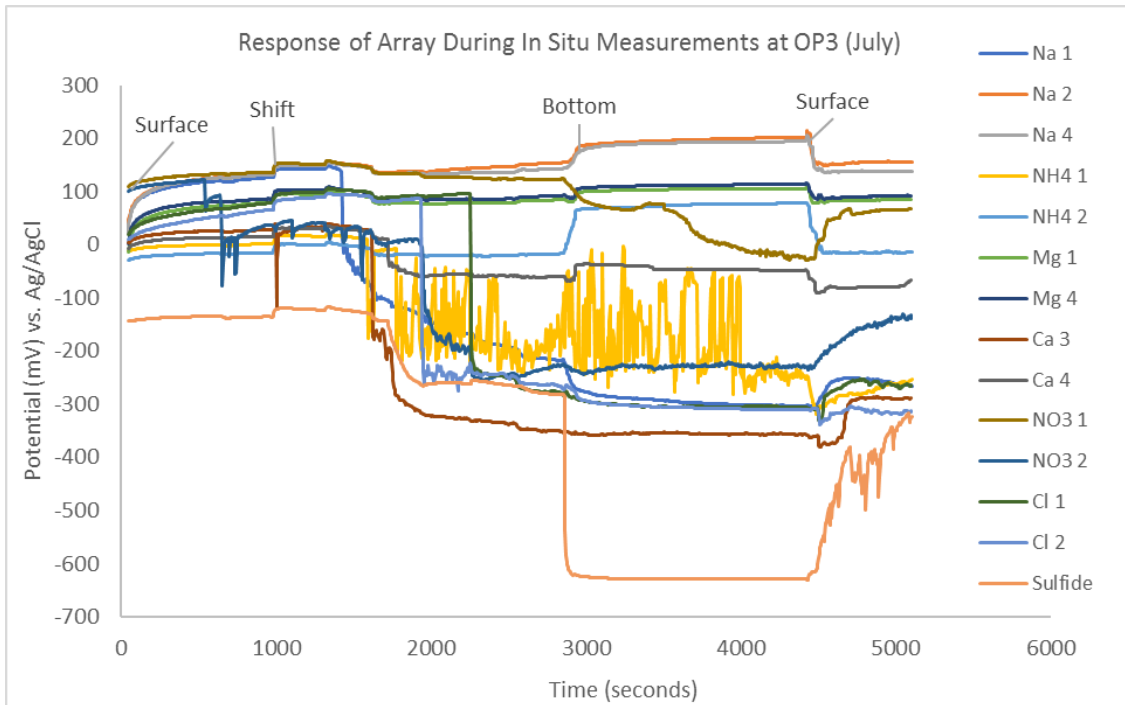


Figure 26. The response of the ISEs during in-situ measurements at OP3 (southern basin, July)

The temperature probe that was attached to the array recorded temperature. The recorded temperature is plotted as a function of depth in Figure X. The temperature was relatively constant between 0 and 3 meters. There was a sharp decrease in temperature in the bottom 4 meters of the pond from 28° to about 15°C. It was important to record temperature to

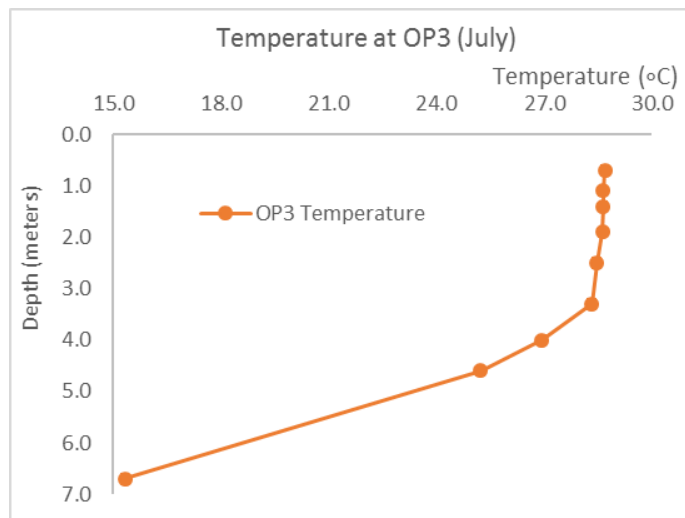


Figure 27. The recorded temperature as a function of depth at OP3 (July).

gain information about stratification in the water column and, more importantly, to convert the ISE response at different temperatures to the expected response at the calibration temperature.

2b. Electrode adjustments: Sulfide ISE characterization and pressure conditioning of electrodes

After observing permanent potential changes in the ISEs during field deployment and unexpected response of the sulfide electrode to other ions like chloride, it was necessary to modify the custom ISEs and further characterize the mixed response of the sulfide electrode. The sulfide electrode was calibrated with standard additions of Na₂S in three different background solutions: deionized water, 0.1 M NaCl and a 1:10 diluted seawater solution (See Table 4 in the Experimental Section for contents of seawater simulant). The calibrations in Figure 28 demonstrate that the intercept was not affected much by the different background solutions. A change of 10 mV in the intercept is equivalent to less than a 1% error. The slope differed by about 6 mV between the water and salt backgrounds. This is also a relatively small magnitude because a decade change in concentration is expected to be ~30 mV, and the desired accuracy is on the scale of an order of magnitude. One should also note that the slopes are all approximately -70 mV per decade while the expected slope is -30 mV per decade for the S²⁻ ion. The expected slopes are for calibrations at highly alkaline pH values (10-14), as suggested by the manufacturer. All the solutions tested were at neutral pH, as was expected in the pond and other natural water sources.

Earlier testing under pressure in the lab indicated that the calibration curves of the ISEs changed less after being exposed to pressure a second and third time compared to the first exposure to pressure (See Figure 15 in Experimental Section 2d). Based on these results, I decided to “pressure condition” the new array of ISEs to prepare them for the field in hopes that the depth of the pond would cause further physical changes to the electrodes. Of the many ISEs that were constructed, the ones that experienced the smallest changes in their slopes and intercepts after the third pressure test were chosen for the field expedition (See Table 5 for results of pressure conditioning).

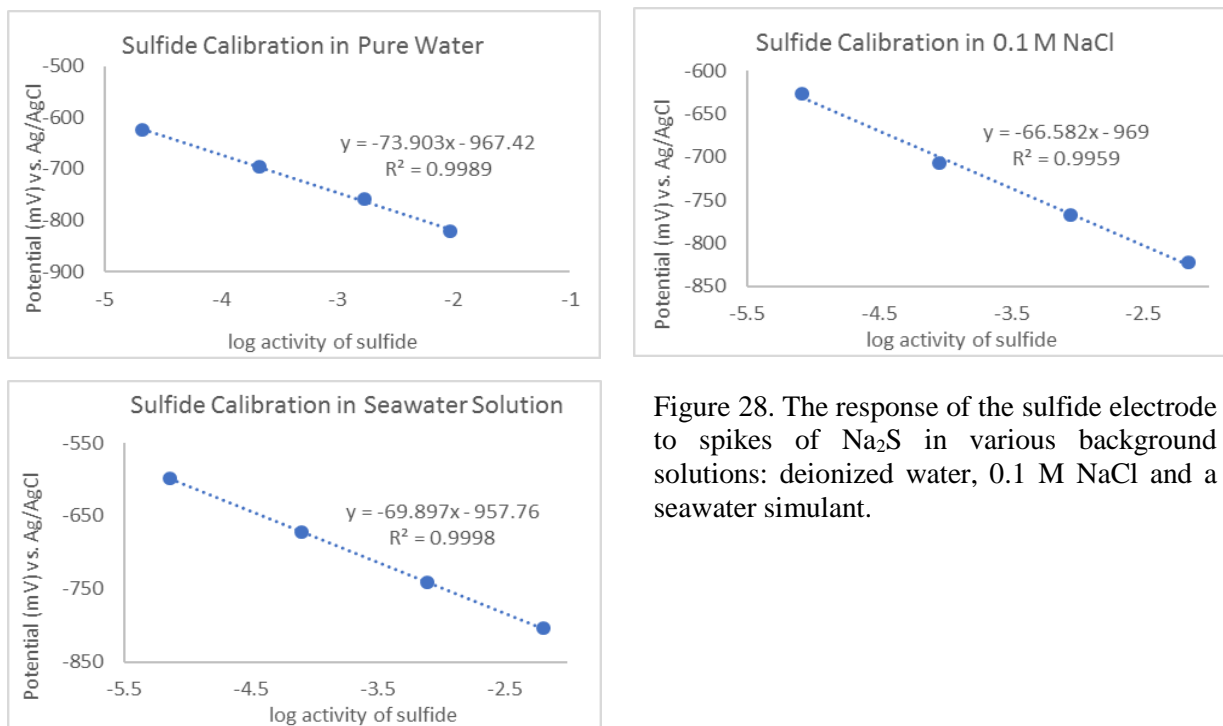


Figure 28. The response of the sulfide electrode to spikes of Na_2S in various background solutions: deionized water, 0.1 M NaCl and a seawater simulant.

2c. Second expedition: August 28th, 2016

I performed calibrations of the ISEs in the field before in-situ measurements and at the end of the day after completing in-situ measurements, in the order of OP3 followed by measurements at OP1. The response during these calibrations is shown in Supplemental Figure 41, and the calibration curves for each ISE are listed in Table 13. The difference between the two calibrations demonstrates which electrodes experienced major changes due to exposure to the environment during in-situ measurements. For example, the Na^+ ISEs had very large changes in their slopes and stopped behaving as cation-selective electrodes. Cl^- ISE #4 was much noisier during calibration 2 than during calibration 1, and all the anion-selective electrodes experienced significant changes in their calibrations. For all the electrodes, the R^2 value was not as close to 1 after in-situ measurements, but were still highly linear and at least 0.94 for most of the ISEs.

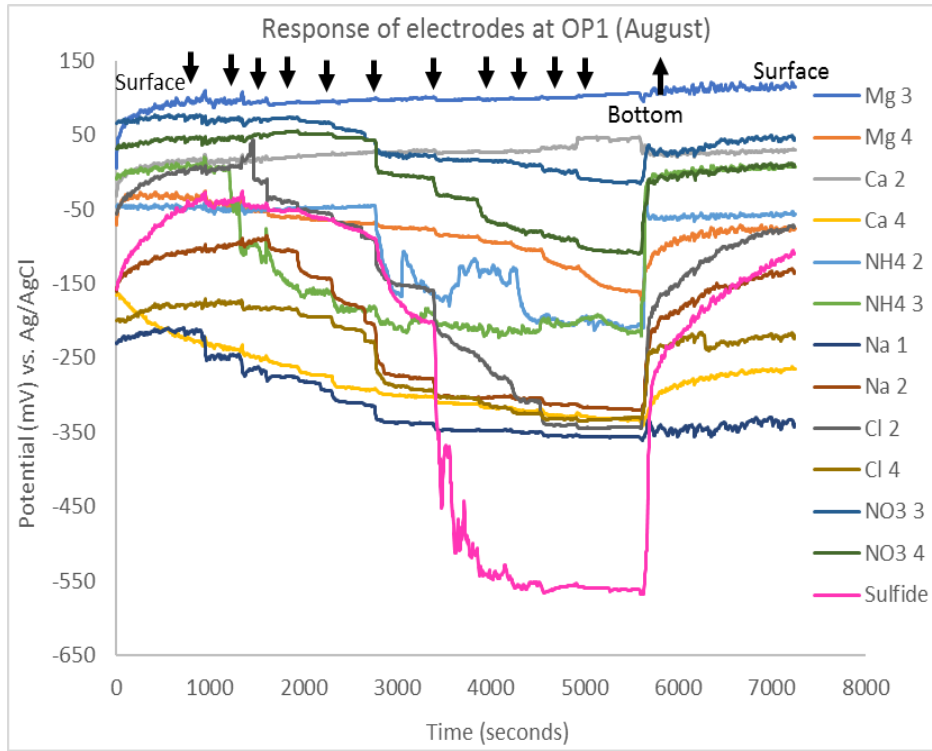
Any electrodes that changed significantly and were no longer working as a typical ISE were excluded from the data processing of calculating the concentrations of ion at OP1 and OP3. In the cases where both electrodes of one type worked well before and after field deployment, such as the NH_4^+ ISEs, the data from both ISEs in both calibrations were averaged to determine the concentrations. If the changes in the intercepts were moderate, such as a change of about 40 mV in the Mg 3 electrode, the first calibration was used to interpret data from OP3, the first site, and then the second calibration was used to interpret OP1 in-situ data.

Table 13. The linear fits of the calibrations before and after in-situ measurements in the field in August.

ISE Name	Calibration before in-situ <i>(slopes and intercepts in mV)</i>	Calibration after in-situ <i>(slopes and intercepts in mV)</i>
Mg 3	$y = 33.6x + 273$ $R^2 = 0.995$	$y = 32.0x + 234$ $R^2 = 0.988$
Mg 4	$y = 34.0x + 301$ $R^2 = 0.997$	$y = 10.8x - 8.8$ $R^2 = 0.904$
Ca 2	$y = 48.9x + 261$ $R^2 = 0.995$	$y = 48.5x + 244$ $R^2 = 0.946$
Ca 4	$y = 46.0x + 221$ $R^2 = 0.948$	$y = 27.3x + 20.5$ $R^2 = 0.981$
NH4 2	$y = 48.4x + 189$ $R^2 = 0.993$	$y = 46.6x + 145$ $R^2 = 0.988$
NH4 3	$y = 60.6x + 277$ $R^2 = 0.991$	$y = 60.1x + 266$ $R^2 = 0.988$
Na 1	$y = 42.4x + 167$ $R^2 = 0.965$	$y = -17.2x - 15.4$ $R^2 = 0.972$
Na 2	$y = 39.3x + 142$ $R^2 = 0.951$	$y = 1.5x + 49.9$ $R^2 = 0.055$
Cl 2	$y = -57.0x - 25.3$ $R^2 = 0.995$	$y = -38.0x - 17.1$ $R^2 = 0.944$
Cl 4	$y = -53.7x - 43.8$ $R^2 = 0.991$	$y = -49.2x - 227$ $R^2 = 0.974$
NO3 3	$y = -39.9x + 65.7$ $R^2 = 0.998$	$y = -46.8x - 6.4$ $R^2 = 0.982$
NO3 4	$y = -37.9x + 87.3$ $R^2 = 0.992$	$y = -46.2x - 21.6$ $R^2 = 0.979$

Note: y represents the measured potential vs. a Ag/AgCl reference and x is the log of the activity of the primary ion.

a



b

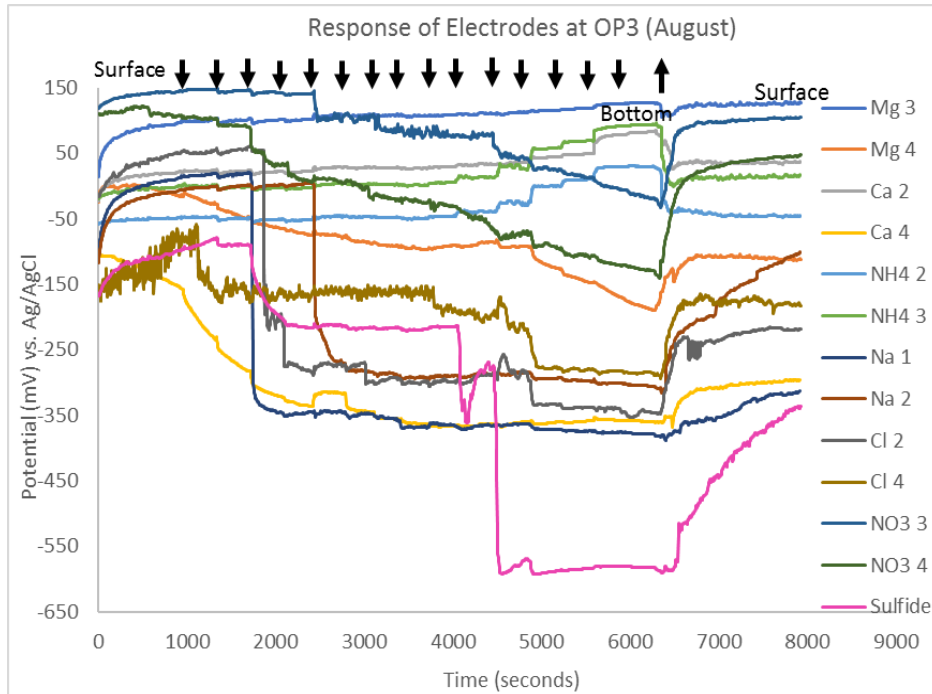


Figure 29. The response of the ND ISEs and the Sulfide ISE during in situ measurement at (a) OP1 and (b) OP3 on August 28th.

Data was first collected at OP3, the deeper basin, followed by collection at OP1 before calibrating again on the dock. An important observation on this day was the high concentration of green algae across the entire pond that made the water extremely turbid. The response of the ISEs during the in-situ measurements is shown above in Figure 29. The arrows indicate each time the array was lowered or raised in the water column. The time at which the array was at the surface or bottom of the basin is also labeled. The “bottom” represents what was thought to be the sediment-water interface due to bubbles coming to the surface, likely from the metal cage dislodging trapped gases in the sediment. These depths were about 4.7 and 6.7 meter for OP1 and OP3, respectively. At both sites, the array was brought back to the surface and allowed to equilibrate again before stopping data collection to determine if the ISEs returned to the original potential they had at the surface. This was true for most of the ISEs. It was not true for the sulfide ISE, especially at OP3. Most of the ISEs responded as expected, with an increase in potential with depth for cation-selective electrodes and a decrease in potential for anion-selective electrodes, especially at OP3 where salinity was known to be higher in bottom layers.¹

The results of the in-situ measurements are summarized below for both basins (Figure 30). The ionic strength of the collected samples was used to calculate activity coefficients and convert activity into concentration. The error bars in the ion graphs are from the error in the linear regression in the calibration curves and the standard deviation in averaging the response of duplicate ISEs. Also note that Figure e is a log plot. Figure 30a shows the temperature as a function of depth, with depth on the y-axis, for both OP1 and OP3. At OP1, the temperature gradually decreased at a constant rate from about 28 to 17°C. At OP3, the temperature remained relatively constant for the first 4 meters of the water column and then decreased at a high rate for the last 2

meters from 25 to 17°C. The error bars represent the standard deviations of temperature at that depth ($n \geq 20$).

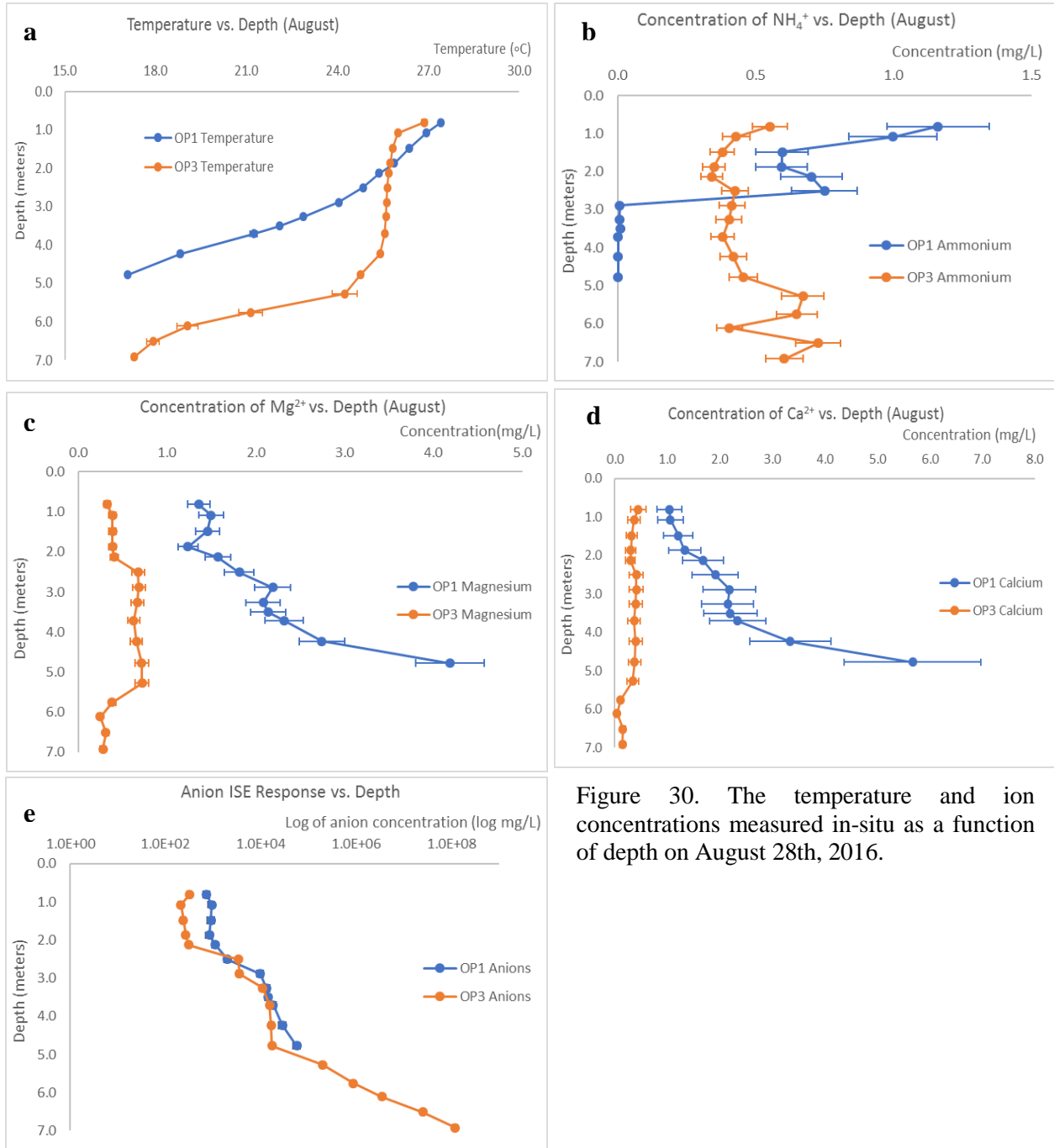


Figure 30. The temperature and ion concentrations measured in-situ as a function of depth on August 28th, 2016.

Figure 30b demonstrates the difference in ammonium trends at OP1 and OP3. At OP1, ammonium was present in the upper part of the pond, but was not detectable and below $0.1 \mu\text{M}$ for the deeper part of the water column. At OP3, ammonium was constant throughout the water column. Figure 30c and Figure 30d demonstrate similar trends between the behavior of Ca^{2+} and Mg^{2+} . Both ions had constant concentrations throughout the water column at OP3, but clearly increased in concentration with depth at OP1. The anion concentration is shown on a logarithmic scale in Figure 30e because of the significant increase in the response of the anion selective electrodes that, when analyzed, translated to large increases in concentration. The concentrations interpreted from all the anion-selective ISEs are not accurate due to the substantial changes in the calibrations shown above in Table 13. It is important to note that the surface temperature and concentrations are similar between OP1 and OP3.

The sulfide electrode reported potentials within the range of -100 to -580 mV. When these potentials were compared to the lab calibrations in seawater simulant (Figure 28), it is clear that these values are not within the range of -600 to -800 mV for activities of sulfide tested. During field calibrations, chloride concentrations in the seawater simulant solutions of up to $\sim 0.2 \text{ M}$ only decrease the potential of the sulfide electrode to only -200 mV.

3. In-lab analysis of Oyster Pond samples

Samples collected from OP3 in July and from both OP1 and OP3 in August were analyzed using the same methods. The analysis of the July samples produced comparable results for the deeper basin, but at a lower resolution, so the figures for July are in the Supplemental section. Below are the summarized results for the August samples, comparing both basins.

3a. Conductivity and pH results

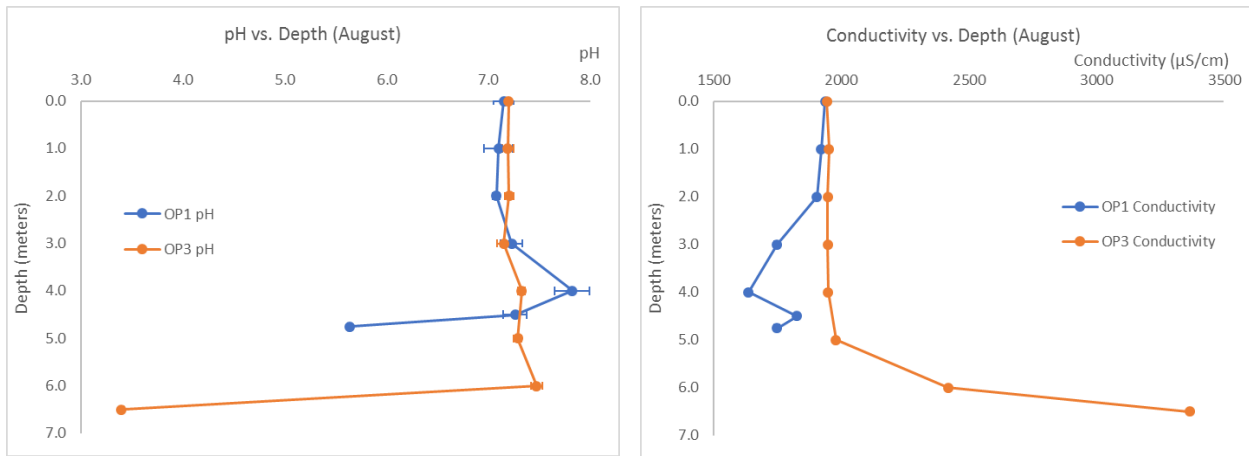


Figure 31. The pH and conductivity results of the samples from OP1 and OP3 collected during the second expedition on August 28, 2016

Figure 31 shows the pH and conductivity as a function of depth. These measurements were taken the laboratory using the samples collected on the first and second expeditions. The error bars in the conductivity and pH plots are the standard deviations of 2 replicate samples (prepared vials 1 and 2). In both basins, the last sample collected was from the sediment water interface. When collecting the samples, it was observed that deeper than 4 meters at OP1 and deeper than 5 meters at OP3, there was a strong sulfidic odor while collecting the samples in bags. The pH and conductivity behave similarly at OP3 in samples from both expeditions (Supplemental Figure 42 and Figure 31). On the second expedition, samples from both basins were collected. At both OP1

and OP3, the pH sharply decreased at the sediment-water interface, but the pH was much lower at the bottom of OP3, at a pH of 3.4. The pH at the bottom of the northern basin was 5.6.

3b. ICP-AES results

Like the pH and conductivity results, the results of the samples collected in July and August demonstrate similar trends in concentrations, but the August samples were at a higher resolution (Figure 32a-d). The error bars are a combination of the standard deviation of 6 replicate samples and the errors in the linear regression of the calibrations. The concentrations listed are labeled as “total” because ICP-AES as a technique will measure the concentration of the element regardless of its initial form in solution. The concentration of sodium remained constant throughout the water column at OP1 at about 200-300 mg/L. At OP2, the concentration of sodium was constant for the first 5 meters and then increased at a high rate in the bottom 2 meters of the pond from 300 to 500 mg/L. Potassium, magnesium and calcium share these trends for both basins. Potassium concentrations were about 10.0 mg/L at OP1 and OP3 from 0 to 5 meters, increasing to 20.0 mg/L at the bottom of the southern basin. Magnesium concentrations were 40-50 mg/L throughout the water column at OP1 and the first 5 meters of the southern basin. Magnesium increased with depth in the lower two meters at OP3 up to about 80 mg/L at the sediment water interface. Calcium concentrations were at 15-25 mg/L throughout the water column at OP1 and the first 5 meters of OP3. Calcium also quickly increased in concentration with depth at the bottom of OP3 from 20 to 50 mg/L. For all metals measured, the concentration was similar for both basins at the surface. The errors were also relatively small.

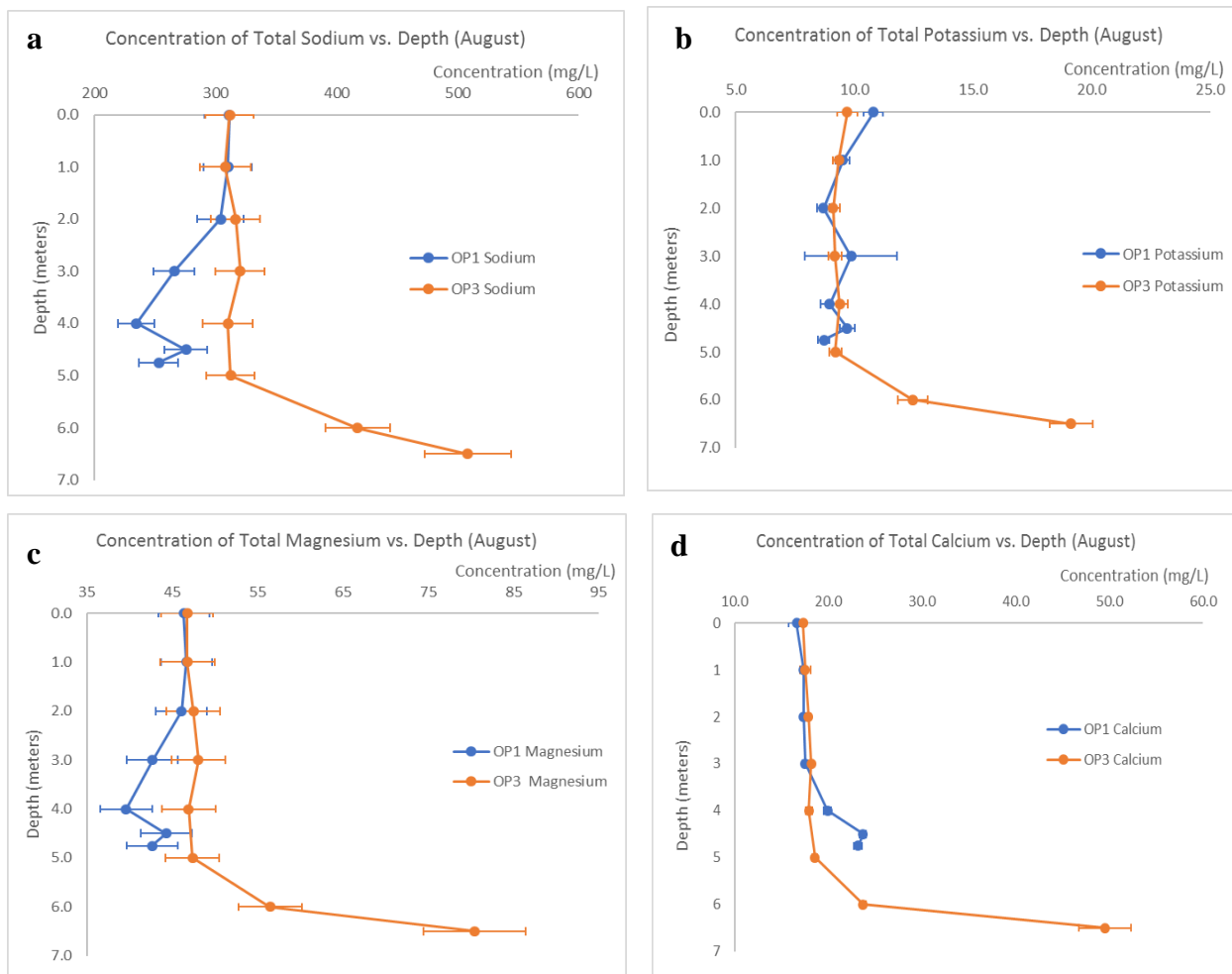


Figure 32. Figure Xa-d. The ICP-AES results of the samples from OP1 and OP3 collected during the second expedition on August 28, 2016.

3c. Ion chromatography results

Ion chromatography was used to measure the concentrations of both cations and anions in the samples for comparison to the in-situ technique and to learn additional chemical information about this pond. Ion chromatography results are excluded for the July samples because they had nearly identical trends and did not provide additional information for this analysis. The concentrations of cations are shown below in Figure 33. The error bars are a combination of the standard deviation of 6 replicate samples and the errors in the linear regression of the calibrations.

The concentrations listed are labeled as “total” because ion chromatography is a separation technique that separates any ion pairs allowing for measurement of the total concentration of that ion in solution, whether it was free or paired. Lithium was excluded because it was at very low levels or not detected in most of the samples. Ammonium was highly variable with large standard deviations because of the presence of ammonia in the deionized water system and therefore, was excluded from the figure.

The analysis demonstrated differing trends among cations. Na^+ increased from 250 to 400-450 mg/L in the first meter at OP1 and then remained relatively constant as a function of depth at concentrations of 300-400 mg/L. At the OP3 site, Na^+ concentrations were constant at depths of 0 to 5 meters at about 300 mg/L and increased with depth from 5-6.5 meters from 300 to 450 mg/L. K^+ was not detected or at very low concentrations in the OP1 samples. In the OP3 samples, K^+ decreased from 2 to nearly 0 mg/L in the first 2 meters, and remains close to 0 mg/L until the last 2 meters of the water column where it increased in concentration to about 10 mg/L. Mg^{2+} and Ca^{2+} shared similar trends in both the northern and southern basins. The concentration of Mg^{2+} was 25-45 mg/L throughout the water column in the northern basin with no significant increase or decrease with depth. Mg^{2+} concentrations were also constant with depth at 25-45 mg/L in the upper 5 meters of the water column at OP3. At greater depths, Mg^{2+} concentrations increased from 30 mg/L to 65 mg/L. Ca^{2+} concentrations were constant with depth at OP1 and in the first 5 meters at OP3 at a concentration of 14-25 mg/L. Like the other cations, Ca^{2+} also increased in concentration with depth from 5 to 6.5 meters at OP3, with a final concentration of nearly 50 mg/L at the bottom.

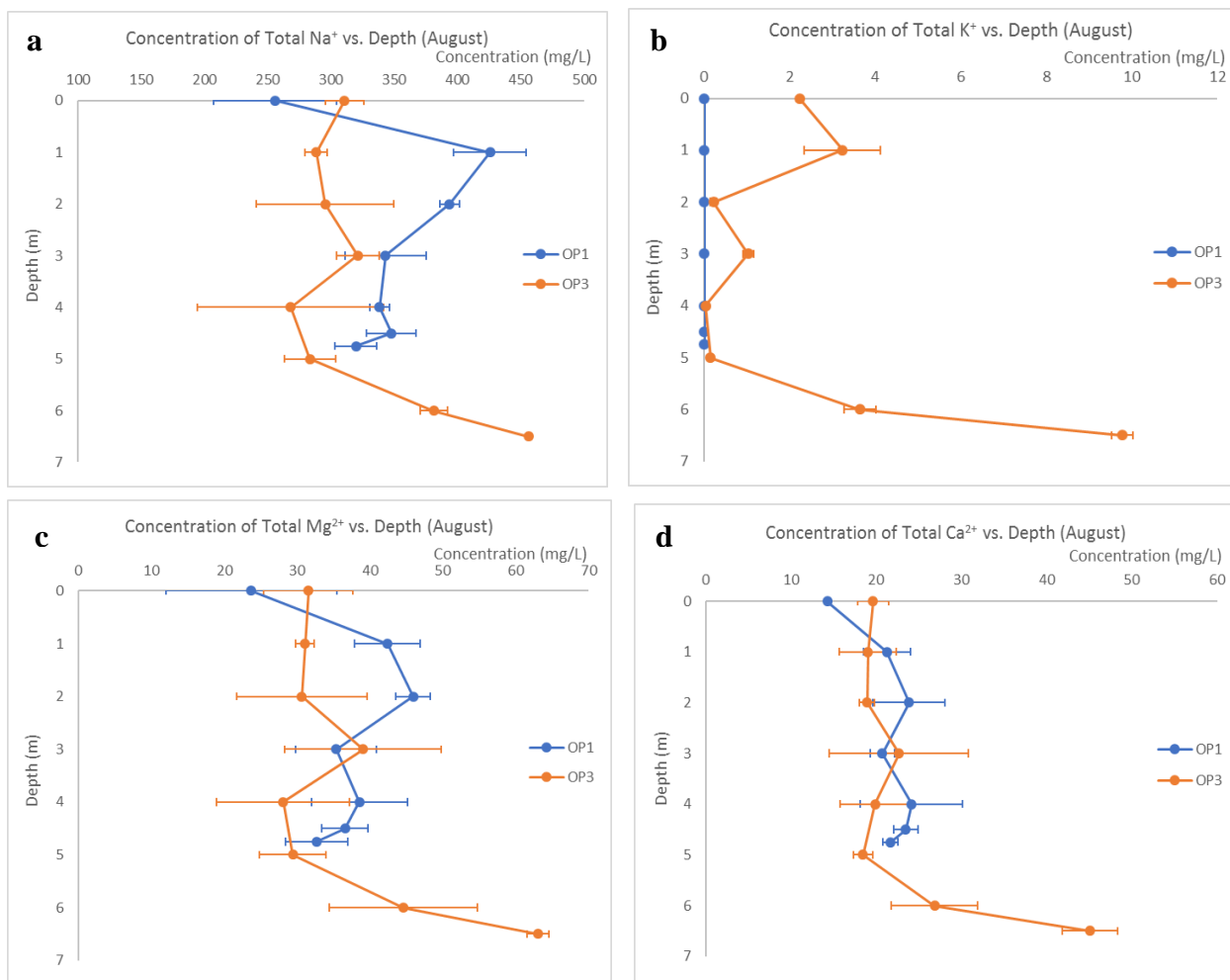


Figure 33. The ion chromatography results of the cations in samples from OP1 and OP3 collected during the first expedition on August 28, 2016.

The trends in concentrations of chloride, bromide and sulfate are shown in Figure 34. The error bars are a combination of the standard deviation of 6 replicate samples and the errors in the linear regression of the calibrations. The chloride concentrations (a) were estimated and do not have error bars because these values exceeded the maximum concentrations in the standards, even with 50x dilution of the samples in the analysis. All the concentrations here are calculated after considering the dilution factor. Other anions were excluded because they were not detected or were associated with large standard deviations. Cl⁻ concentrations were calculated based on the calibrations despite being in concentrations excess of the most concentrated standard, even when

diluted 50x before analysis. Although the concentrations are estimated, they still show similar trends to the concentrations of the cations. Concentrations of chloride were relatively constant with depth in the north basin and in the upper 5 meters of the southern basin and a strong increase in concentration from 5 to 6.5 meters in the southern basin. Br⁻ also demonstrated a similar trend with OP1 and OP3 (0-5 meters) concentrations of about 2.5 mg/L and a clear increase in concentration with depth from 5 to 6.5 meters at OP3 from 2.5 to 3 mg/L. SO₄²⁻ also indicated similar behavior with depth of the sample. The concentrations were 50-100 mg/L in the northern basin and in the upper 6 meters of the southern basin and a strong increase in concentration from 50 to 450 mg/L in the bottom 0.5 meters of OP3.

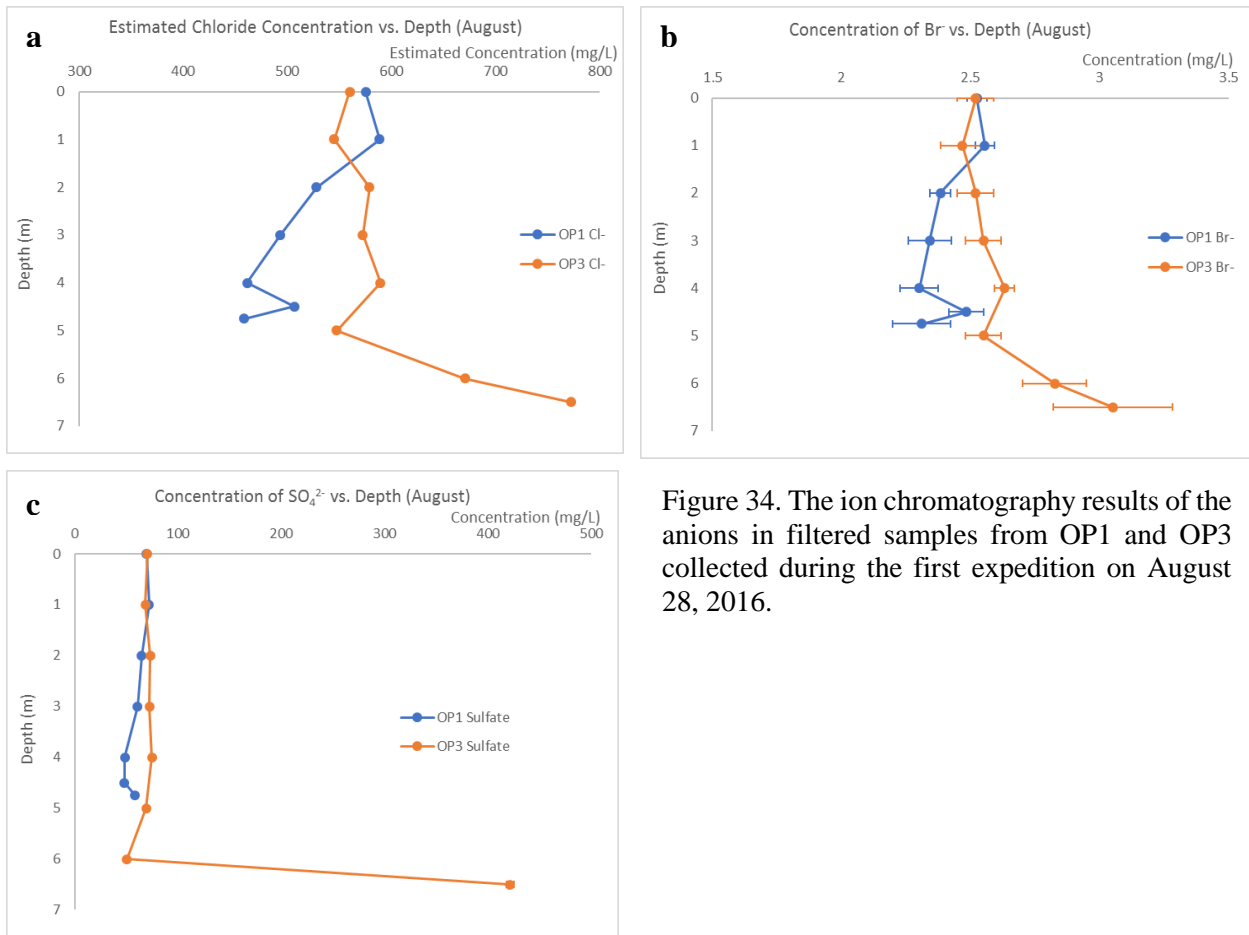


Figure 34. The ion chromatography results of the anions in filtered samples from OP1 and OP3 collected during the first expedition on August 28, 2016.

Discussion

1. Evaluation of tests for “field-readiness”

Tests under the conditions expected in the field, both at Oyster Pond and the Skaftá lakes, were performed to evaluate the viability of the ND ISEs as in-situ electrodes. In the natural environment, solutions with multiple ionic species are expected, so the tests in sulfidic and anoxic solutions were all performed with mixed spiking solutions or background solutions of multiple ions, such as Na^+ , K^+ , Mg^{2+} , Ca^{2+} , Cl^- , acetate and sulfide. Regardless of the presence of other ionic species, the cation-selective ISEs responded selectively to their primary ion under all conditions. The Cl^- ISEs did not perform as well, confirming the observed lack of selectivity seen in further experiments (See Table 12).

Tests of the ISEs in the presence of sulfide were performed because of previous reports of sulfide at the bottom of Oyster Pond and in multiple samples from the Skaftá lakes.^{1,2,6} Calibrations in water and in 1 mM H_2S were similar for the cation-selective ISEs (Table 9), demonstrating that the presence of H_2S did not affect their ability to behave as ideal ion-selective electrodes. The Cl^- -selective electrodes, however, did not behave as typical ion-selective electrodes in a background of 1 mM H_2S . The calibration had a positive slope with increasing chloride activity and a R^2 value of 0.368, rather than a negative linear slope as predicted by the Nernst Equation.¹⁴ In other tests, the Cl^- -selective electrodes also failed. When in a mixed chloride salt background, additions of Na_2S caused the Cl^- -selective electrodes to drift to lower potentials and to become noisier. In contrast, the Mg^{2+} and Ca^{2+} ISEs remained at a stable potential with no effects due to increased sodium or sulfide in the solution to concentrations as high as 0.1 mM. A similar difference was seen between the cation-selective ISEs and the Cl^- ISEs in drift tests (Figure 23). These responses may indicate “poisoning” of the Cl^- ISEs, especially because they did not calibrate properly after

initial exposure to sulfide in the first test and one of the two Cl^- ISEs drifted excessively in a chloride solution without any sulfide present. The poisoning may be in the form of diffusion of sulfide into the membrane, associating with the lipophilic salts in the membrane, or by continuous reaction with the membrane surface as seen in the literature.²³

The bottom layers of Oyster Pond and the Skaftá lakes were also observed to be anoxic.^{1,2} Under anoxic conditions, all the ISEs tested performed well. They had nearly Nernstian slopes for their calibrations in both an oxygenated and deoxygenated solution (

Table 10). Their E° values did not change more than 10 mV, demonstrating consistency of calibrations between the two different environments. For all the ISEs, oxygen did not affect the potentials of the membrane.

After confirming that the cation ISEs were selective and were not affected by sulfidic or anoxic conditions, they were tested in real samples collected from the West and East Skaftá lakes. The results demonstrated that the Na^+ ISEs accurately reported the concentration of Na^+ but that there were some issues with cross-selectivity of the K^+ , Mg^{2+} and Ca^{2+} ISEs, causing these ISEs to overestimate the concentrations of their respective cations (

Table 11). In general, the ISEs did respond sensitively to changes in concentration between the two samples, showing that they are still useful for in-situ profiling of a stratified water column because they report relative differences in ion concentrations very well. The concentrations in the samples were also near the limits of detection for some of the ISEs possibly causing the erroneous response, but this would not be an issue for Oyster Pond, a brackish pond of higher salinity,¹ and detection of ions in the concentrated particles of Enceladus's plumes.^{26,27} It is also possible that further calculations and research could have been performed to further characterize the cross-selectivity of these ISEs and use it as an asset in a multi-electrode array along with an artificial neural network, also known as an "electronic tongue."²⁸

It is known that seawater is a major source of water for Oyster Pond,¹ so it was necessary to then characterize the ND ISEs and the commercial sulfide electrode in mixed solutions and seawater simulants. Selectivity coefficients in the literature may be found for the chosen membrane

cocktails,^{14,17-21} but new coefficients were calculated for this specific ISE construction method. The chosen method was the Fixed Interference Method¹⁴ because it best simulates the expected environment in that an interferent, especially NaCl, would be in a high concentration such as 0.1 M,¹⁵ while the primary ion changes in concentration. The Fixed Interference selectivity tests demonstrated high selectivity of the cation ISEs for their primary ion, as was expected from previous calibrations with mixed spiking solutions. The Ca²⁺ ISEs were not as selective as the Na⁺, Mg²⁺ and NH₄⁺ ISEs. The Cl⁻ and NO₃⁻ ISEs were not as selective as any of the cation-selective ISEs, a common pattern that was appearing throughout the testing and characterization of these electrodes, demonstrating the need for further research on improving selectivity of anion ISEs in natural and environmentally-relevant solutions.

Calibration of the array of ND ISEs (Na⁺, Mg²⁺, Ca²⁺, NH₄⁺, Cl⁻, NO₃⁻) and the sulfide electrode with calibration solutions mimicking the contents of seawater produced excellent results with working ranges of the electrodes well exceeding the ranges of concentrations expected in the brackish coastal pond. The sulfide electrode did respond in this calibration, most likely due to chloride binding with silver ions in the crystal membrane. The directions from the manufacturer recommend polishing, especially after exposure to complex solutions, which is a downfall of this solid-surface ISE because it is not practical to polish the ISE in the field. All the ISEs responded within 1 minute, which was ideal for in-situ deployment, allowing the ISEs to respond quickly upon lowering to the appropriate depth. This fast of a response time could also allow the ISEs to be lowered continuously at a controlled rate with a more advanced pulley system. The use of the modified Deep-Sea Lawson Box during this calibration demonstrated the success of the modification of electronics and readiness for field deployment. It is also important to note that these results were repeatable in the field during calibrations on the Oyster Pond dock.

2. In-situ measurements at Oyster Pond

The completion of tests in sulfidic, anoxic, real samples and seawater-like solutions, along with successful calibrations with the appropriate salinity ranges and modified electronics confirmed that the ISEs were ready for field deployment. Calibration on the dock during the first field expedition was comparable to the calibration in the lab. The response during field measurements in the deeper, southern basin of Oyster Pond, however, was poor. Many of the electrodes “broke” in the way that they exhibited erratic noise and large potential shifts not associated with changing the depth of the array (Figure 26). Erratic noise could be attributed to a break in the membrane or back of the electrode, causing liquid to leak into the electrode and encountering the silver wire. The large potential shifts were attributed to changes in the E° term of the Nernst equation. This term encompasses many potentials, such as the junction potentials within the reference electrode, potentials of the interior components of the ISE, and the boundary and diffusion potentials of the ISE membrane.^{13,14} I suspect that at one point during the in-situ measurements that the reference electrode junction potential changed because all the ISEs experienced the same shift. At other times, there were large potential shifts in individual electrodes, which can be attributed to a change within the ISE or on the ISE membrane, likely because of changing pressure that shifted the internal components or the membrane.

Despite the shifts in potential, it was clear that the ISEs did respond to increasing salinity with depth. The suspected stratification of ions was confirmed by temperature measurements. A constant temperature in the upper 4 meters of the water column in Oyster Pond’s southern basin (OP3) indicated that these waters were well mixed in July. The bottom (4-6.5 meters) was clearly a separate water layer as indicated by a strong decrease in temperature with depth not present in

the upper part of the water column. These results align with previous studies in the 1960s and 1990s that identified a separate water layer at the bottom of the southern basin under both high and low salinity conditions.¹

This first expedition acted as an initial test of the array, identifying what modifications and further characterization needed to be performed. The shifts in potential of many of the ND ISEs led to the incorporation of “pressure conditioning” into the construction method before the next field expedition in August. This greatly improved the performance of the ISEs during the second expedition in August. Most of the cation ISEs worked well and collected reliable data about the activity of ions with depth with reasonable error, except that both Na⁺ ISEs broke. Future work with such an array would benefit from increasing the number of constructed ISEs prior to assembling the array and carrying out tests to choose the best ISEs. In this study, I was only able to prepare four ISEs of each type and then chose the best two after pressure testing. The anion ISEs however, probably would not have benefited from increasing the number of electrodes prepared and tested prior to fieldwork because of sulfide-exposure related failures. Both the Cl⁻ and the NO₃⁻ ISEs responded with very large potential decreases at the bottom of both OP1 and OP3. From earlier tests in sulfidic solutions it was evident that the Cl⁻ ISEs began to fail and were possibly poisoned. This must have occurred with all the anion ND ISEs in the array because the chloride concentrations of $\sim 1 \times 10^5$ to $\sim 1 \times 10^8$ mg/L (Figure 30) are not realistic for the bottoms of the basins, and the calibrations before and after in-situ measurements were significantly different for all the anion ND ISEs (Table 13).

The commercial sulfide electrode was characterized further because of its response to chloride. Calibrations in pure water, 0.1 M NaCl and seawater simulant had similar slopes and intercepts. Most interestingly, the slope was consistently ~ 70 mV. This may have been a response

to HS^- , which is the predominant form of hydrogen sulfide at neutral pH because the first deprotonation of H_2S has a pK_a of 6.9.²⁹ This response of the sulfide electrode at neutral pH further decreases the viability of this commercial electrode for in-situ measurements.

In the field, the response of the sulfide electrode only reach -580 mV in the bottom layers of the pond, where sulfide was expected from previous studies¹ and detected by smell from samples. This is outside of the working range of -600 to -800 mV for activities of $\sim 10^{-6}$ to $\sim 10^{-2}$ M in seawater simulant (Figure 28). This demonstrates that the sulfide concentration may have been less than $\sim 5 \mu\text{M}$, or that the matrix of the natural pond water strongly affected the potential of the sulfide electrode. It is not likely that high chloride concentrations were responsible for potentials as low as -580 mV because field calibrations with maximum chloride concentrations that well exceeded those expected in the pond resulted in potentials only as low as -200 mV. The low concentration of HS^- and S^{2-} may have caused the lack of response if the pH was low enough for the primary form to be H_2S . At a pH of 5.6 and 3.4 in the northern and southern basins, respectively, it is likely that H_2S was the primary form because its pK_{a1} is 6.9.²⁹

3. Comparison of in-situ to in-lab analysis and interpretation of Oyster Pond's chemistry

The second expedition resulted in successful collection of in-situ depth profiles for multiple ions and temperature, and samples in both the northern (OP1) and southern (OP3) basins of Oyster Pond. The in-lab analysis along with the known characteristics of this model system allow for a comprehensive evaluation of the in-situ array and interpretation of the chemical state of the pond.

The in-situ array was successful in detected ammonium in contrast to ICP-AES which does not have the ability to measure ammonium by nature, and in contrast to IC which had large standard

deviations between replicate ammonium measurements due to presence of ammonia in the deionized water used for blanks and dilutions. Ammonium was only present in concentrations of up to ~1.3 mg/L, much less than the ~28 mg/L detected by Howes and Hart at the bottom of the southern basin in 1996, but the algal bloom occurring at this time may have caused the consumption of ammonium, a form of nitrogen easily taken up by algae and plankton.¹ It is also possible that recent management of the pond to lower the salinity has allowed for less severe stratification and more diffusion of ammonium out of the bottom layer and into the rest of the water column.

As discussed earlier, the anion ISEs, including the ND ISEs and the commercial sulfide ISE, did not successfully report accurate concentrations. Analysis by ion chromatography also resulted in inaccurate chloride data. Despite the 50:1 dilution of the samples and the wide range of the calibration, chloride was still in much greater concentrations than the most concentrated standard. One could have analyzed all the samples at two different dilutions, but this is tedious and not practical to just obtain chloride concentrations. The IC results only allowed for an estimate of chloride. Future research on the exposure of the anion ND ISEs to sulfide or further characterization of the mixed response of the sulfide ISE to both chloride and sulfide may prove more useful than having to rely on multiple dilutions and analysis by ion chromatography, since in-situ analysis doesn't require storage, filtration and dilution of samples.

All three methods allowed for measurements of calcium and magnesium, but with contrasting results. The data for each ion in each basin are shown for all three methods in Figure 35a-d. The error bars for the IC and ICP data are standard deviations of six replicate measurements. The ISE error is a relative error calculated from the error in the linear fit of the calibration curves.

The upper x-axis shown concentrations for the IC and ICP-AES data, and the lower axis is for the ISE data.

Comparing *a* to *b* and *c* to *d* clearly shows that magnesium and calcium behave similarly with depth in both the northern basin and the southern basin. It is also clear that in all four plots, concentrations calculated from ICP-AES and IC data are consistent with each other, showing the same trends at similar concentrations. Magnesium and calcium seem to both stay constant with depth in the northern basin and upper 4 meters of the southern basin, but increase with depth from 4 to 6.5 meters in the southern basin. The ISE data, however, show the opposite trend for both ions in both basins. Also, the concentrations of calcium and magnesium were found to be about 10 times less for the potentiometric method. Lower concentrations in a potentiometric measurement is expected because this method only measures “free” and unpaired ions,^{11,13,14} as labeled on the bottom axes.

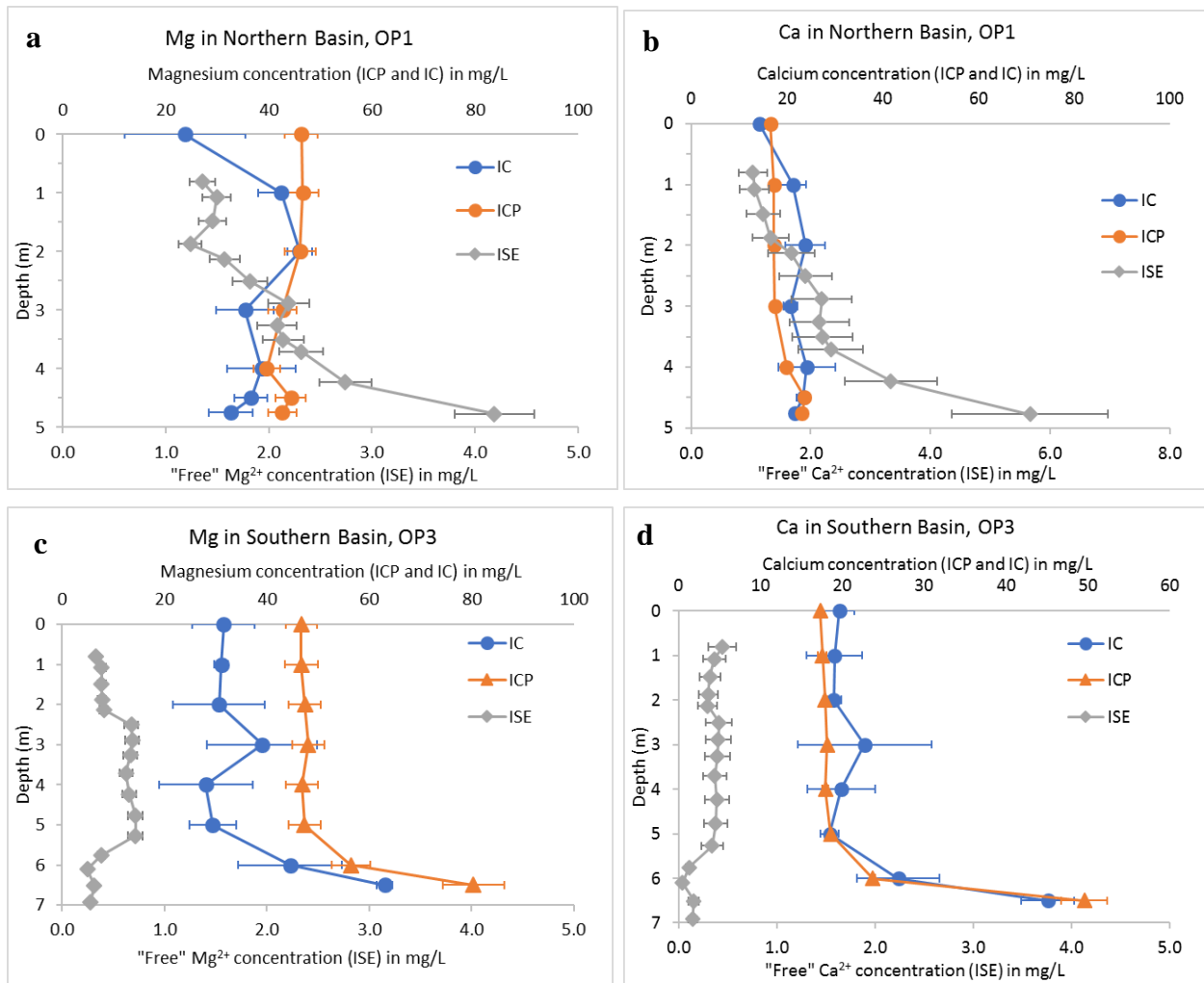


Figure 35. The comparison of the three methods: ion chromatography (IC), inductively-coupled plasma atomic emission spectroscopy (ICP-AES) and potentiometry with ion-selective electrodes (ISEs) for measurement of magnesium and calcium in the two basins of Oyster Pond.

The discrepancy between the ISE results and the IC and ICP results requires further explanation. It is not likely that cross selectivity for Na^+ or K^+ caused the response in the ISEs, because the ICP and IC data confirm that Na^+ and K^+ are constant with depth at OP1 and increases with depth at OP3, the opposite trend that the ISEs shown for Mg^{2+} and Ca^{2+} . It may be explained by ion-pairing of Ca^{2+} and Mg^{2+} with other ions, especially sulfate, in the water column. It is known that 8% of carbonate, 81% of bicarbonate and ~ 39% of sulfate ions exist as ion pairs with Ca^{2+} and Mg^{2+} in seawater.²⁵ Therefore, in the presence of excess sulfate, ion pairing should be more

prevalent and seen as a decrease in free ion activity of Mg^{2+} and Ca^{2+} . In Table 14 are the maximum concentrations for each ion found using ion chromatography. The maximum concentrations correspond to the concentrations at the deepest point of each basin, as expected because of the density of seawater compared to freshwater and observed stratification in earlier studies.^{1,15} If one assumes 100% ion-pairing between sulfate and the two cations, and equal pairing with each cation, it is clear that free Ca^{2+} and Mg^{2+} are in excess at the bottom of the northern basin, but free sulfate is in excess at the bottom of the southern basin while Ca^{2+} and Mg^{2+} are present only as ion pairs, agreeing with the observed trends for “free” Ca^{2+} and Mg^{2+} at OP1 and OP3.

Table 14. The concentrations of sulfate, magnesium and calcium ions in the two basins of Oyster Pond

	Northern Basin (OP1)			Southern Basin (OP3)		
Ion	SO_4^{2-}	Mg^{2+}	Ca^{2+}	SO_4^{2-}	Mg^{2+}	Ca^{2+}
mg/L	58	32	20	421	63	45
mmol/L	0.60	1.32	0.50	4.38	2.59	1.12
Excess (mmol/L)		1.01	0.20	0.67		

The disagreement between the ISE data and the sample analysis demonstrate one of the advantages of the ND ISEs. They responded selectively to the primary ion, especially for Ca^{2+} and Mg^{2+} , and demonstrated the behavior of the free, unpaired ions. This information is important for understanding the availability of ions in the water column and the equilibria of key geochemical species such as sulfate.

These new data on stratification of inorganic ions, ammonium, sulfide, and other ions in this pond will benefit both the scientific community and the local community. Knowledge about mixing in the pond and the depth of the anoxic layer is important to the local conservation organization, Oyster Pond Environmental Trust, Inc. (OPET), that has been monitoring the pond

for the past few decades. It will inform OPET about the availability of the benthic environment to fish and other aquatic life and the patterns of salinity throughout the water column. Development of novel in-situ instrumentation for this anoxic and sulfidic environment will provide new tools for the scientific community to use in extreme environments like the Skaftá lakes or Enceladus could identify ions out of equilibrium, such as sulfate which could serve as an energy source for bacteria and other organisms.²

Conclusion

Many advantages of the Newly Designed ISEs were discovered through this study. They were selective for the primary analyte ion, especially Ca^{2+} and Mg^{2+} , allowing for observation of ion pairing and chemical disequilibria. Ammonium concentrations were observed directly, and excess sulfate could be identified indirectly using ISEs. Both of these ions are important nutrient and energy sources for organisms on Earth.^{1,2,6} The ammonium data was also much more reliable from the ISEs compared to the IC system because of ammonia in the water blanks. Another success of this study was the vast improvement of the ISEs upon pressure conditioning that allowed for increased robustness and performance. The ability of these ISEs to withstand changes in pressure is an excellent and necessary trait for extreme environment analyses, such as at the bottom of the Skaftá lakes or in a variable environment like space. Recently published data on the success of a solid-supported polymeric membrane ISE at high pressures of 105 bar also point to the promise of ISEs in extreme environmental analysis.³⁰

The standard techniques in the lab do not measure the “free” activity of the ions in the natural environment, and are much more tedious in sample collection, storage, preparation and analysis. In contrast, the ISEs allowed for nearly instantaneous data collection in the real environment without the need for any sample alteration. The amount of work needed for in-situ data collection could further be reduced through programming an algorithm to instantaneously process the observed potentials into concentrations if a CTD (Conductivity-Temperature-Depth) probe accompanied the array.

It is possible that some of the chemical species could have changed in concentration after sampling. To confirm that the differences seen were due to the differences between in-situ and in-lab analysis and not just the difference between potentiometry, spectroscopy and chromatography,

it would be necessary to perform an in-lab analysis on the samples using the ND ISEs. These measurements have been planned and will be presented in a future publication.

Despite these successes, the ND ISEs need to be improved for future use in extreme environmental analysis. No accurate anion data was collected, likely because of the interference and possible poisoning due to sulfide. The failure of some the cation ISEs demonstrated the need for producing larger batches of the ISEs before choosing the best ones for in-situ analysis. One could also combat this probability of failure by including more ISEs of each type. This could easily be done by using existing potentiometers, such as the expanded version of the EMF16 (Lawson Labs, Inc.) with 96 channels instead of 16.

The Newly-Designed ISEs show a great amount of potential in future use for chemical analysis of extreme environments. The ISEs could withstand sulfidic, anoxic, and high pressure conditions, like those expected in the Skaftá lakes and in the subsurface oceans of Enceladus and Europa. Their fast response and selectivity allowed for fast, real-time in-situ data collection. In the Skaftá lakes, these characteristics would be necessary to observe high resolution changes in ion concentrations with depth.

Supplemental

WCL electrodes characterization

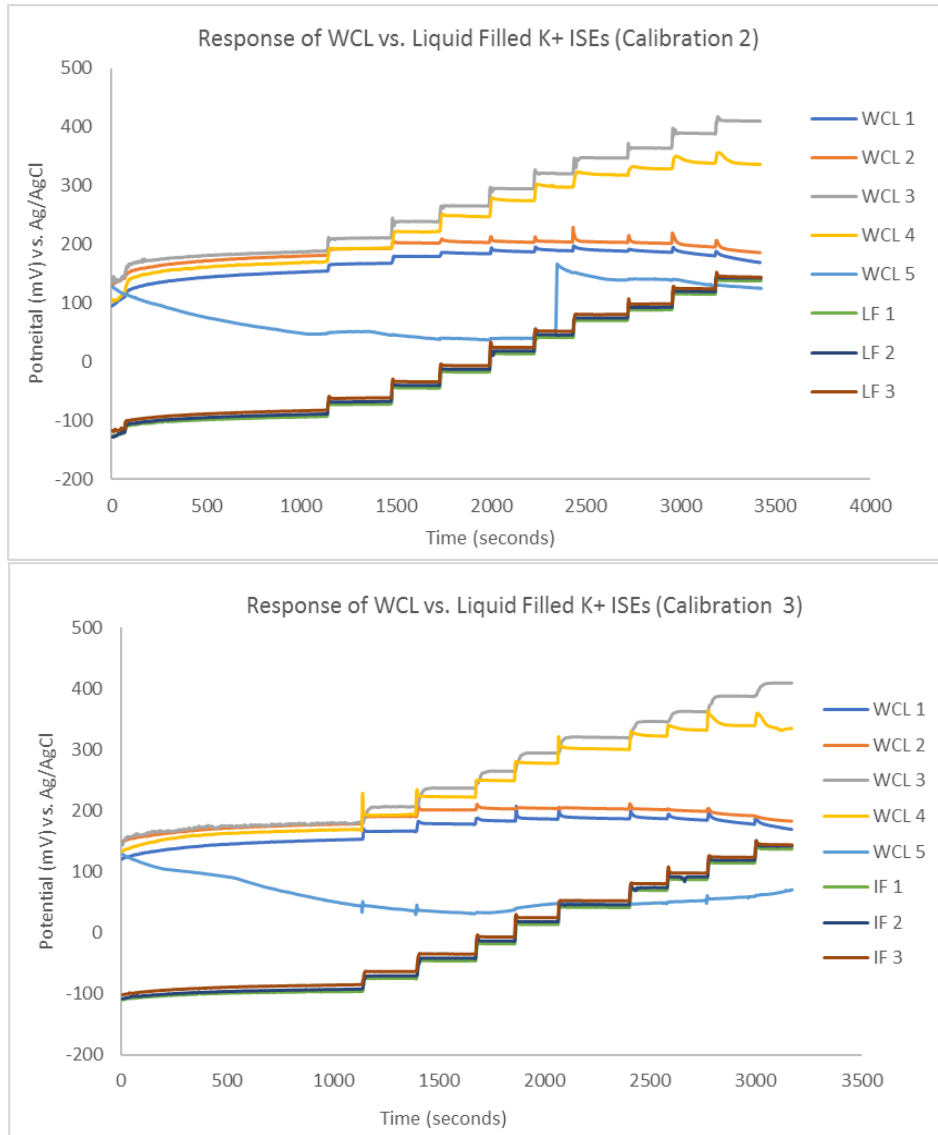


Figure 36. The response of WCL and Liquid Filled K⁺- ISEs with the same membrane components to additions of KCl to deionized water. These two calibrations were conducted within the same day, after Calibration 1 in Figure 10.

Calibrations under expected conditions and Skaftá sample measurements

Table 15. The calibrations of the ND ISEs before and after the measurement of each Skaftá sample

ISE name	Before West Sample		After West Sample		Before East Sample		After East Sample	
	Slope (mV)	Intercept (mV)	Slope (mV)	Intercept (mV)	Slope (mV)	Intercept (mV)	Slope (mV)	Intercept (mV)
Na 1	47.7	254.7	51.2	268.8	51.7	249.3	50.1	245.6
Na 2	50.9	292.6	54.3	305.2	55.6	302.4	54.2	297.0
K 1	24.7	123.2	23.4	118.8	30.0	140.2	29.7	140.3
K 2	24.8	125.2	23.5	125.7	31.0	150.6	30.3	150.4
K 3	26.2	129.4	25.0	130.2	30.7	127.0	31.3	134.1
Mg 1	21.7	145.6	22.8	152.2	23.1	150.6	20.4	144.1
Mg 2	21.6	135.5	23.1	142.3	23.0	142.9	20.4	136.7
Mg 3	21.1	133.2	22.8	136.9	22.7	139.7	20.4	133.5
Ca 1	18.8	131.6	17.8	133.4	20.2	134.9	20.4	137.9
Ca 2	17.9	130.2	17.0	132.2	19.0	134.5	19.8	139.0
Ca 3	18.8	141.7	18.0	143.6	20.0	145.9	20.6	148.6

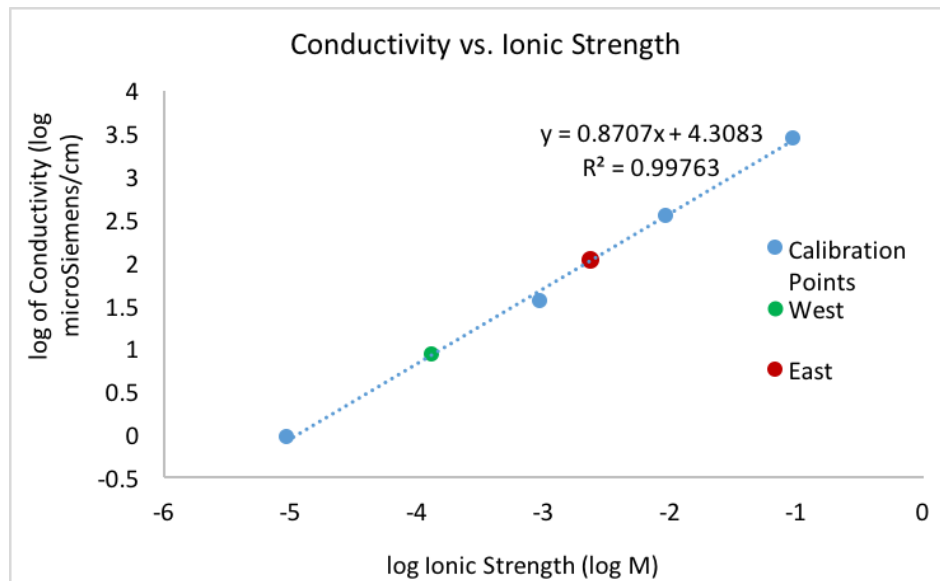


Figure 37. The calibration curve used to determine the ionic strength of the Skaftá samples from their conductivity

ND ISEs characterization

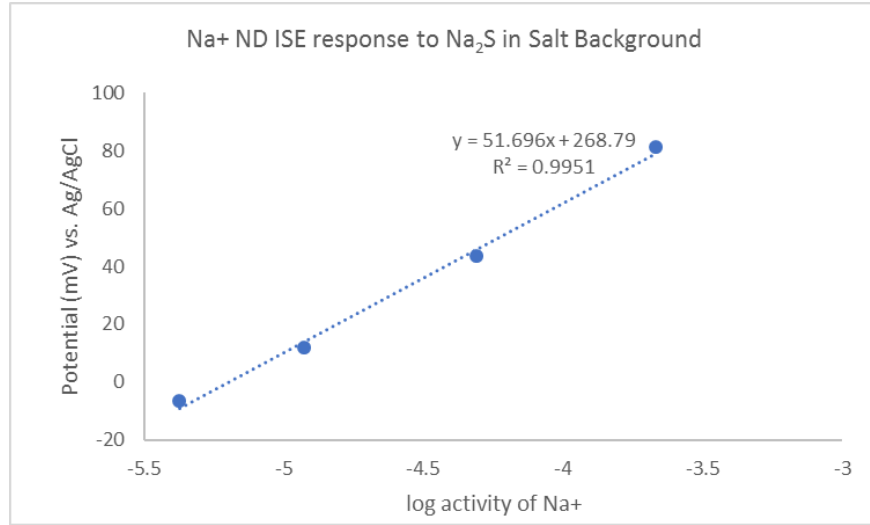


Figure 38. The calibration of the Na⁺ ND ISE with Na₂S in a background of 0.1 mM MgCl₂, CaCl₂ and KCl in water.

In-situ measurements at Oyster Pond

First expedition: July 29th, 2016

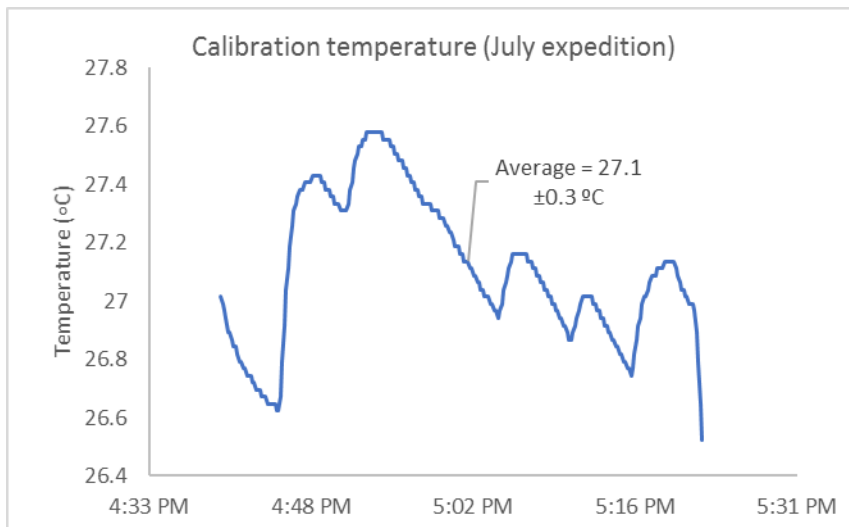


Figure 39. Temperature measurements during the calibration on the dock at Oyster Pond.

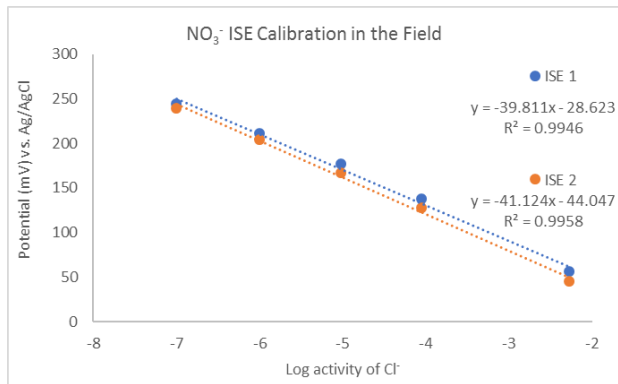
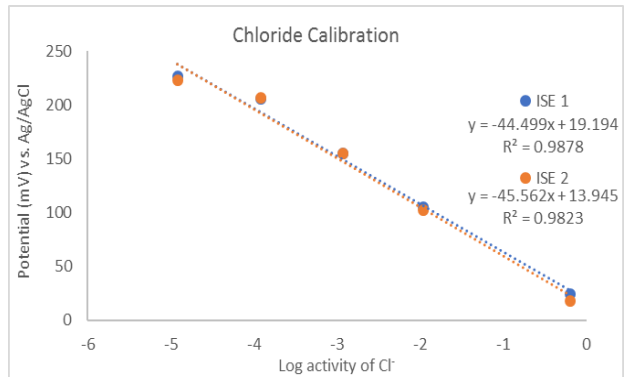
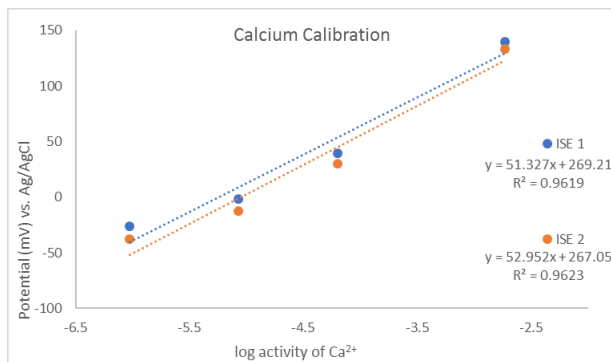
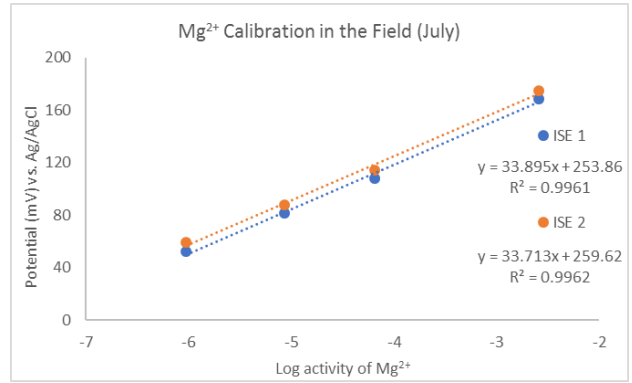
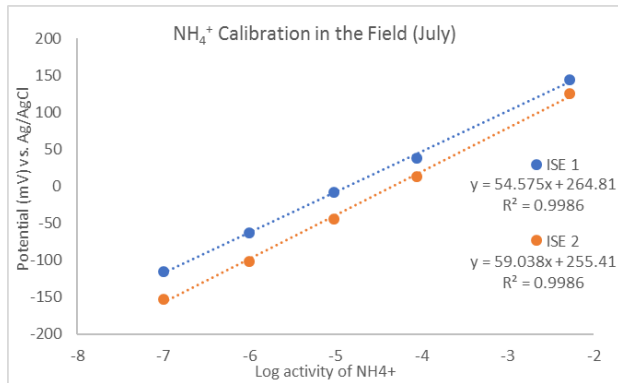


Figure 40. The calibration curves associated with the in-field calibration on July 29th, 2016.

Second expedition: August 28th, 2016

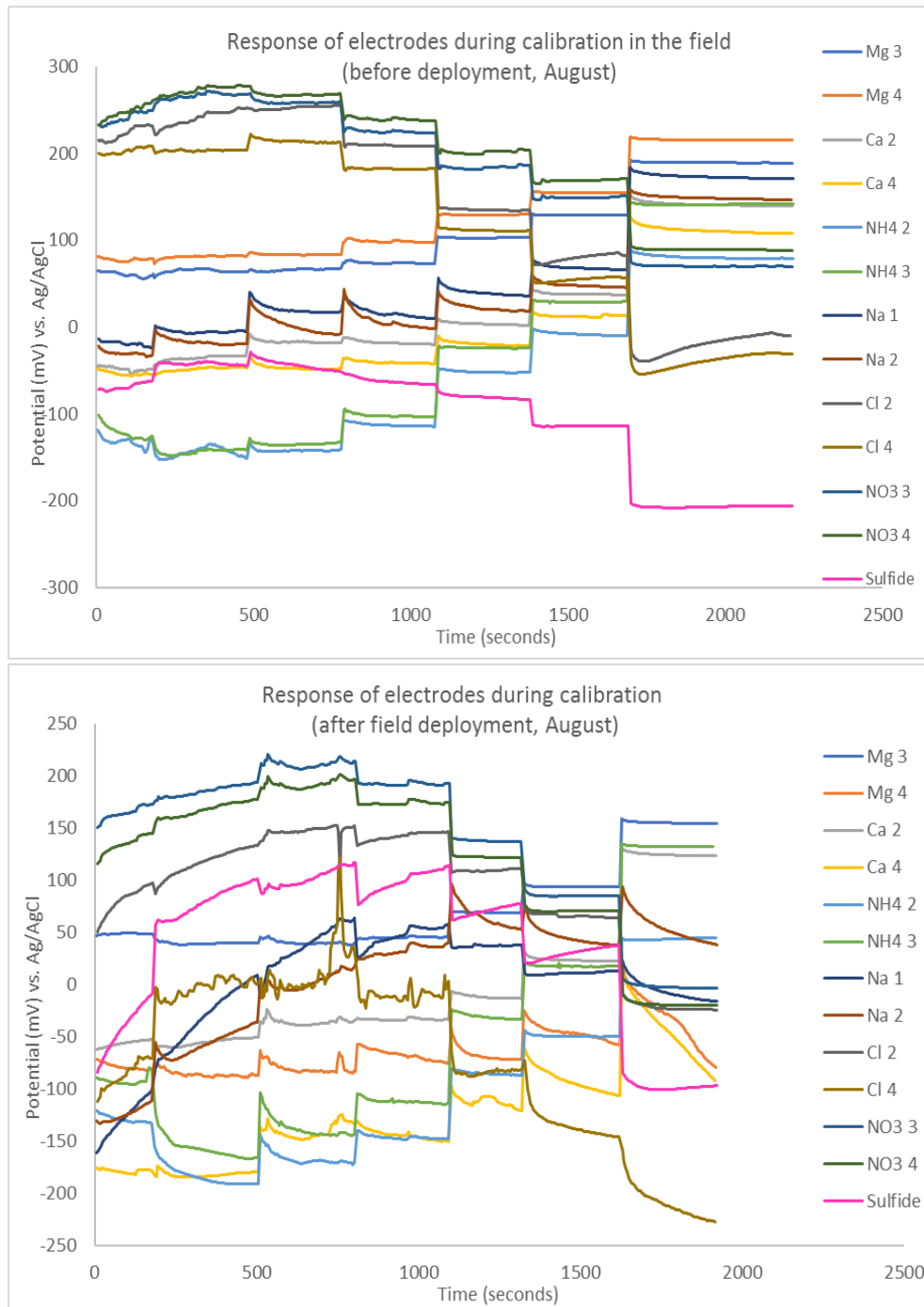


Figure 41. The response of the array of ISEs during calibrations in the field on the dock both before and after deployment (August)

In-lab analysis of samples

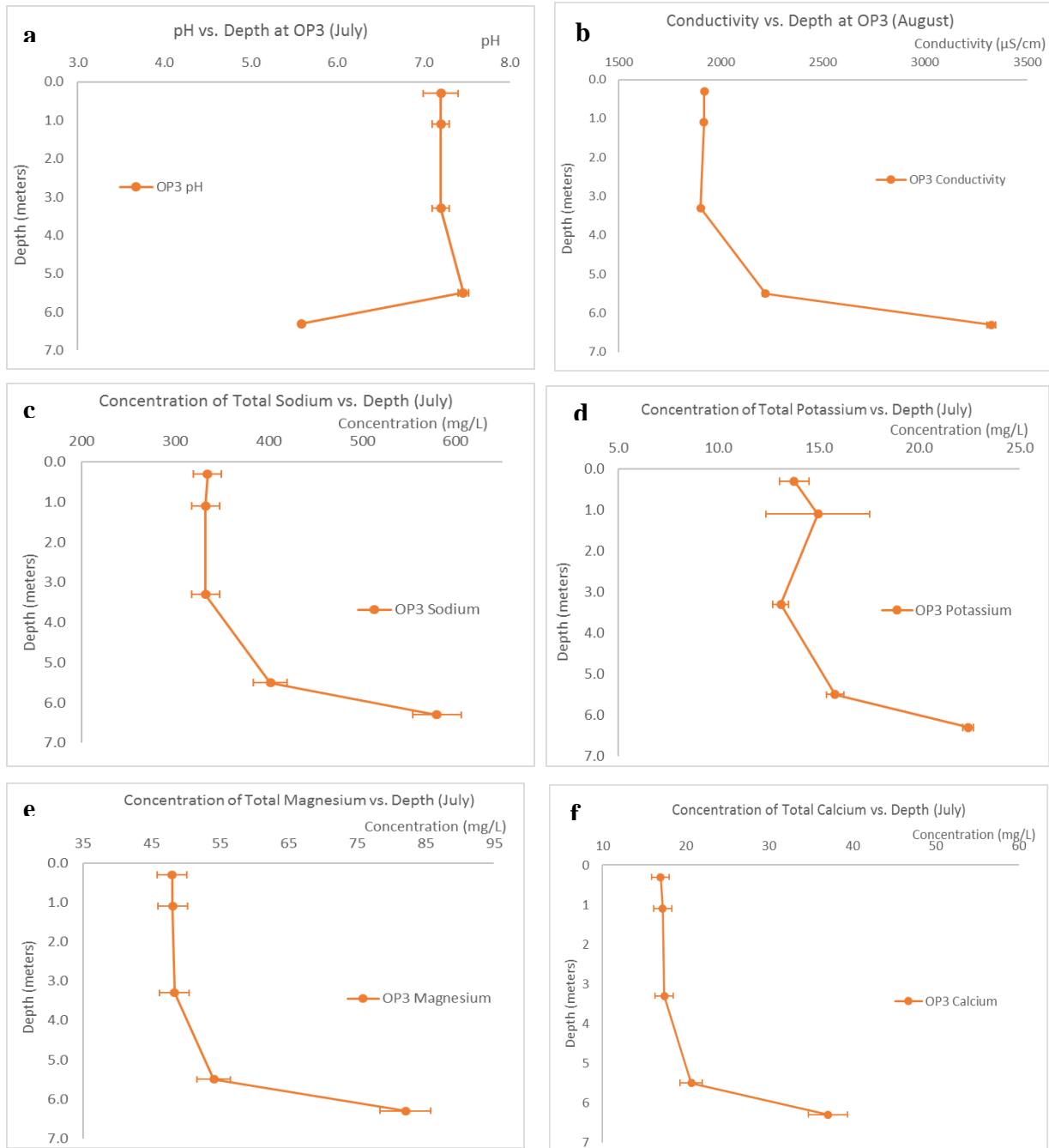


Figure 42. The (a) pH, (b) conductivity and (c-f) ICP-AES results of the samples from OP3 collected during the first expedition on July 29, 2016.

The error bars in the conductivity and pH plots are the standard deviations of 2 replicate samples (prepared vials 1 and 2). The error bars in c-f are a combination of the standard deviation of 6 replicate samples and the errors in the linear regression of the calibrations. The concentrations listed in c-f are labeled as “total” because ICP-AES as a technique will measure the concentration of the element regardless of its initial form in solution.

Table of Figures

Figure 1. An artist's rendering of the global ocean and hydrothermal activity of Enceladus, a moon of Saturn (Courtesy of NASA/JPL-Caltech).....	7
Figure 2. Ion profiles in the East Skaftá Lake. The triangle and circle represent 2 different boreholes. Sulfate is in black. SiO ₂ , Na ⁺ and Cl ⁻ are in gray. (Adapted from Marteinson et al. 2013).	8
Figure 3. A map showing the location of Oyster Pond in southern Massachusetts and details of the connection to the Vineyard Sound through the Lagoon and Trunk River. (Courtesy of OPET, Inc.) ⁸	9
Figure 4. Historic anoxia in Oyster Pond. The diagram on the right was under lower salinity conditions. (From Emery et al. 1997)	10
Figure 5. The salinity as a function of depth in the southern, deeper basin of Oyster Pond as reported by Emery (1964) and Howes and Hart (1988-1991). ¹	10
Figure 6. A typical potentiometric setup and details of a polymeric membrane-based ion-selective electrode. (Adapted from Harris 2007)	12
Figure 7. Components of the membrane potential. A graph of the components of the measured potential in an ion-selective electrode (top) and a detailed schematic of the components of a polymeric membrane (bottom). ^{11,13}	14
Figure 8. A cross-section of a typical ion-selective electrode	20
Figure 9. A cross-section of a WCL ion-selective electrode (Kounaves et al. 2009).....	21
Figure 10. The response of K ⁺ -selective WCL and Liquid-Filled ISEs made with the same membrane components.	22
Figure 11. The calibration curves of potassium-selective WCL and LF ISEs with the same membranes in a pure KCl and water solution.....	22
Figure 12. The calibration plot of cation-selective WCL ISEs using spikes of KCl performed immediately prior to and after exposing the electrodes to high pressures.	24
Figure 13. A schematic of the Newly Designed ISEs.....	25
Figure 14. A photo depicting the dimensions of the ND ISEs.....	25
Figure 15. The response curves and calibrations of Na ⁺ -selective ND ISEs to spikes of NaCl in water.....	26
Figure 16. Testing the temperature probe in the lab	32
Figure 17 . The experimental setup including the modified potentiometer in a waterproof aluminum chassis and array of electrodes during field calibrations	34
Figure 18 . The inner tube and pulley system that supported the cage, electronics and electrodes during in-situ measurements	35
Figure 19. A topographical map of Oyster Pond and the sampling sites (Modified from Emery et al.)	36

Figure 20. Fieldmaster® Water Sampler	37
Figure 21. The calibration of the conductivity probe using the known ionic strength of the ICP standards	38
Figure 22. The calibration plots for the response of the ICP-AES to the prepared standards	39
Figure 23. The effects of sulfide on the ND ISEs.....	44
Figure 24. The response during calibration of the array of ND ISEs prepared for fieldwork in Oyster Pond using seawater simulants.....	47
Figure 25. The response curve and calibration plot of the ND ISEs during calibration on the dock on July 29th, 2016.....	49
Figure 26. The response of the ISEs during in-situ measurements at OP3 (southern basin, July).....	51
Figure 27. The recorded temperature as a function of depth at OP3 (July).....	51
Figure 28. The response of the sulfide electrode to spikes of Na ₂ S in various background solutions: deionized water, 0.1 M NaCl and a seawater simulant.....	53
Figure 29. The response of the ND ISEs and the Sulfide ISE during in situ measurement at (a) OP1 and (b) OP3 on August 28th.	55
Figure 30. The temperature and ion concentrations measured in-situ as a function of depth on August 28th, 2016.....	57
Figure 31. The pH and conductivity results of the samples from OP1 and OP3 collected during the second expedition on August 28, 2016.....	59
Figure 32. Figure Xa-d. The ICP-AES results of the samples from OP1 and OP3 collected during the second expedition on August 28, 2016.	61
Figure 33. The ion chromatography results of the cations in samples from OP1 and OP3 collected during the first expedition on August 28, 2016.	63
Figure 34. The ion chromatography results of the anions in filtered samples from OP1 and OP3 collected during the first expedition on August 28, 2016.	64
Figure 35. The comparison of the three methods: ion chromatography (IC), inductively-coupled plasma atomic emission spectroscopy (ICP-AES) and potentiometry with ion-selective electrodes (ISEs) for measurement of magnesium and calcium in the two basins of Oyster Pond.	73
Figure 36. The response of WCL and Liquid Filled K ⁺ - ISEs with the same membrane components to additions of KCl to deionized water. These two calibrations were conducted within the same day, after Calibration 1 in Figure 10.	78
Figure 37. The calibration curve used to determine the ionic strength of the Skaftá samples from their conductivity	79
Figure 38. The calibration of the Na ⁺ ND ISE with Na ₂ S in a background of 0.1 mM MgCl ₂ , CaCl ₂ and KCl in water.....	80
Figure 39. Temperature measurements during the calibration on the dock at Oyster Pond.	80
Figure 40. The calibration curves associated with the in-field calibration on July 29th, 2016. ...	81

Figure 41. The response of the array of ISEs during calibrations in the field on the dock both before and after deployment (August) 82

Figure 42. The (a) pH, (b) conductivity and (c-f) ICP-AES results of the samples from OP3 collected during the first expedition on July 29, 2016..... 83

References

- (1) Emery, K. O.; Howes, B. L.; Hart, S. R. *A Coastal Pond Studied by Oceanographic Methods, Epilogue: Oyster Pond - Three Decades of Change*; Oyster Pond Environmental Trust, Inc.: Woods Hole, MA, 1997.
- (2) Gaidos, E.; Marteinsson, V.; Thorsteinsson, T.; Jóhannesson, T.; Rúnarsson, A. R.; Stefansson, A.; Glazer, B.; Lanoil, B.; Skidmore, M.; Han, S.; Miller, M.; Rusch, A.; Foo, W. *ISME J.* **2009**, *3* (4), 486–497.
- (3) Delsemme, A. H. *Am. Sci.* **2001**, *89* (5), 432–442.
- (4) Khan, A. *LA Times*. September 17, 2015.
- (5) Jóhannesson, T.; Thorsteinsson, T.; Stefánsson, A.; Gaidos, E. J.; Einarsson, B. *Geophys. Res. Lett.* **2007**, *34* (19), 1–6.
- (6) Marteinsson, T. V.; Rúnarsson, Á.; Stefánsson, A.; Thorsteinsson, T.; Jóhannesson, T.; Magnússon, S. H.; Reynisson, E.; Einarsson, B.; Wade, N.; Morrison, H. G.; Gaidos, E. *ISME J.* **2013**, 427–437.
- (7) Thorsteinsson, T.; Elefsen, S. O.; Gaidos, E.; Lanoil, B.; Jóhannesson, T.; Kjartansson, V.; Marteinsson, V. P.; Stefansson, A.; Thorsteinsson, T. *JOKULL* **2007**, *57*, 71–82.
- (8) Oyster Pond <http://www.opet.org/> (accessed Sep 13, 2016).
- (9) Kounaves, S. P.; Hecht, M. H.; West, S. J.; Morookian, J.-M.; Young, S. M. M.; Quinn, R.; Grunthaler, P.; Wen, X.; Weilert, M.; Cable, C. A.; Fisher, A.; Gospodinova, K.; Kapit, J.; Stroble, S.; Hsu, P.-C.; Clark, B. C.; Ming, D. W.; Smith, P. H. *J. Geophys. Res.* **2009**, *114*, E00A19.
- (10) Bobacka, J.; Ivaska, A.; Lewenstam, A. *Chem. Rev.* **2008**, *108* (2), 329–351.
- (11) Harris, D. C. *Quantitative Chemical Analysis*, Seventh.; W.H. Freeman and Company: New York, 2007.
- (12) Bakker, E.; Bühlmann, P.; Pretsch, E. *Chem. Rev.* **1997**, *97* (8), 3083–3132.
- (13) Mikhelson, K. N. *Ion-Selective Electrodes*; Springer: St. Petersburg, 2013.
- (14) Bakker, E. *Anal. Chem.* **1997**, *69* (6), 1061–1069.
- (15) In *Seawater: It's Composition, Properties and Behaviour*; Suckow, M. A., Weisbroth, S. H., Franklin, C. L., Eds.; Elsevier Ltd., 1995; pp 29–38.
- (16) Agustsdottir, A. M.; Brantley, S. L. *J. Geophys. Res.* **1994**, *99* (B5), 9505–9522.
- (17) Gehrig, P.; Rusterholz, B.; Simon, W. *Chimia (Aarau)*. **1989**, *43* (12), 377–379.
- (18) Rothmaier, M.; Simon, W. *Anal. Chim. Acta* **1993**, *271* (1), 135–141.
- (19) O'Donnell, J.; Li, H.; Rusterholz, B.; Pedrazza, U.; Simon, W. *Anal. Chim. Acta* **1993**, *281* (1), 129–134.
- (20) Qin, W.; Zwickl, T.; Pretsch, E. *Anal. Chem.* **2000**, *72* (14), 3236–3240.
- (21) Cadogan, A. M.; Diamond, D.; Smyth, M. R.; Deasy, M.; McKervey, M. A.; Harris, S. J. *Analyst* **1989**, *114* (12), 1551.
- (22) US Department of Commerce, N. O. and A. A. .
- (23) Athavale, R.; Kokorite, I.; Dinkel, C.; Bakker, E.; Wehrli, B.; Crespo, G. A.; Brand, A. *Anal. Chem.* **2015**, *87* (24), 11990–11997.
- (24) Pond Sampling Map <http://www.opet.org/water-quality-monitoring-map.html> (accessed Sep 20, 2016).
- (25) Pytkowicz, R. M.; Hawley, J. E. *Limnol. Oceanogr.* **1974**, *19* (March), 223–234.
- (26) Waite, J. H.; Combi, M. R.; Ip, W.-H.; Cravens, T. E.; McNutt, R. L.; Kasprzak, W.; Yelle, R.; Luhmann, J.; Niemann, H.; Gell, D.; Magee, B.; Fletcher, G.; Lunine, J.; Tseng, W.-L.

- Science* **2006**, *311* (5766), 1419–1422.
- (27) Hansen, C. J.; Esposito, L.; Stewart, A. I. F.; Colwell, J.; Hendrix, A.; Pryor, W.; Shemansky, D.; West, R. *Science* **2006**, *311* (5766), 1422–1425.
- (28) De Marco, R.; Clarke, G.; Pejic, B. *Electroanalysis* **2007**, *19* (19–20), 1987–2001.
- (29) *CRC Handbook of Chemistry and Physics*, 84th Edition.; 2004.
- (30) Weber, A. W.; O’Neil, G. D.; Kounaves, S. P. *Anal. Chem.* **2017**, acs.analchem.7b00366.